Calcium imaging of the entire muscle system of *Hydra* reveals extensive cellular multifunctionality

John Szymanski

Submitted in partial fulfillment of the
Requirements for the degree of
Doctor of Philosophy
under the Executive Committee
of the Graduate School of Arts and Sciences

COLUMBIA UNIVERSITY

2018

ABSTRACT

Calcium imaging of the entire muscle system of *Hydra*
reveals extensive cellular multifunctionality

John Szymanski

Hydra vulgaris is a cnidarian species with a life cycle containing only a polyp stage, and a simple body plan in which ectodermal and endodermal epitheliomuscular cells play many roles. One of their roles is to act as muscle—these two epithelia generate motion of the polyp by exerting contractile force through myonemes. The function of this musculature was studied on a system scale using whole-animal calcium imaging to measure functional activity in all epitheliomuscular cells simultaneously. This approach maps the diversity of functional activation patterns underlying the behavior of *Hydra*, and reveals that individual epitheliomuscular cells participate in multiple patterns using at least two different types of calcium signaling that propagate at vastly different speeds. These studies establish the functional basis for the epithelial muscle systems of Cnidaria, revealing new operational principles and deep evolutionary ties to mechanisms of contractile activity that exist elsewhere in Metazoa.

CONTENTS

LIST OF CHARTS, GRAPHS, ILLUSTRATIONS

ACKNOWLEDGEMENTS

This work would not have been possible without the support of a community of colleagues in the *Hydra* field and here in the Yuste lab, and I would like to express my gratitude to everyone I have had the chance to work with along the way, and to my advisor Rafael Yuste for giving me the opportunity to do this work. Particular thanks must be paid to Rob Steele, Celina Juliano, Charles David, and Stefan Siebert, who all welcomed us into the Hydra research community and shared their wealth of knowledge and tools – we would have been lost without their cheerful and gracious welcome to the field. Thanks also to the rest of the team we have collaborated with on our work supported by DARPA. The professors on my thesis committee each played an important role in honing this work: Darcy Kelley, Raju Tomer, Ozgur Sahin, and Roberto Etchenique. My colleagues in the Integrated Program in Cellular Molecular and Biomedical Studies and in the Yuste Lab have been critical to my education and progress as well. I have also been lucky enough to work with some talented undergrads from Columbia and Barnard, and this project was aided particularly by John Wang, Cameron Meyer-Mueller, Jacqueline Ridgely, and Caroline Silverman. I would also like to extend utmost gratitude to my parents Ingrid Gebavi and Bob Szymanski and my sister Katie Szymanski for their inexhaustible support, as well as the rest of my community for weaving me into the web of interdependence without which nothing makes sense. This work was supported by DARPA award DARPA-HR0011-17-C-0026

Of mortal parts and fire eternal
a tiny beast, namesake infernal
manifests its foot and head—
chaos from within is shed

between compartments charges pumped
with excitation, swiftly dumped
thru channels anciently inherent
from atop giants made apparent

lit with arcane apparatis
sub specie aeternitatis
waves and bursts are seen existent
patterns varied yet persistent

through sheets of cells interdependent
with none emerging clear ascendant
coordinate the creature's actions
in pursuit of satisfactions

it spends its days eating crustaceans
and if unhappy with its stations
simply does some somersaults
or on a bubble, quickly vaults

INTRODUCTION

"You can observe a lot by watching."

-Berra

The phylum Cnidaria diverged from its sister group, Bilateria, early in the history of animals, ~750 million years ago, [1] and contains examples of metazoan life that stand in stark contrast to those bilaterally symmetric species that comprise the vast majority of animal models in biology. Within the diversity of Cnidaria, *Hydra vulgaris* is notable for living in freshwater—almost all other cnidarians are marine—and for having a simple life cycle containing only a polyp stage, which has a simple anatomy. The simplicity of *Hydra* presents an opportunity to study its biology on a whole-animal scale, including the relatively fast processes involved in electrical activity of the nervous system and the behavior that it generates, studies which have been recently completed by colleagues in the Yuste Lab. [2], [3] Yet downstream of the firing of neurons, it is the excitation and contraction of muscle that generates behavior. In this study, I address this gap in our knowledge of the neuromuscular system that generates behavior in *Hydra* by performing whole-animal calcium imaging in the epitheliomuscular cells, mapping dynamics in the entire musculature of an animal for the first time. This approach revealed the patterns of contraction that exist in these tissues on a whole-system scale, identifying functional principles of cnidarian epithelial muscle systems, properties of the multiple types of excitatory activity that comprise them, and the ways that these systems compare with other metazoan muscle tissues, shedding light on the evolutionary history of contractile excitation in Metazoa.

Anatomy of Hydra

The *Hydra* polyp has a simple body plan with radial symmetry around an oral-aboral axis. The polyp can range in size from less than 1 mm to over 15 mm, depending on the extent of feeding or starvation, with a maximum size depending on species and temperature. The structure of the polyp consists of ectodermal and endodermal epithelia with a layer of extracellular matrix between them called the mesoglea, which contains mostly fibrous proteins and proteoglycans. [4] The two epithelia and mesoglea form a layered body wall that is continuous throughout the entire polyp, enclosing a gastric cavity within (Fig. 1). The aboral end has a foot, or basal disc, which can attach the polyp to a substrate. Moving orally, the peduncle region is followed by the body column, from which buds are produced to reproduce asexually. Further toward the oral end, tentacles are attached in a ring around the base of the hypostome, the cone-shaped region with the mouth at the oral tip. The mouth is closed by septate junctions between cells which are disconnected by muscle contraction to open the mouth. [5] Interspersed between the epithelial cells is a lineage of interstitial cells that comprises 80% of the cells in *Hydra*, including multipotent stem cells, various types of neurons arranged in a nerve net, gland cells, and the stinging cnidocytes that give Cnidaria its name. [6] The epitheliomuscular cells play many roles in the animal, combining physiological and muscular functions that are separated into different tissues in most animals. Ectodermal epitheliomuscular cells function as the protective skin of the polyp, and their large vacuoles have a role in osmoregulation, while endodermal epitheliomuscular cells serve to digest food. Both epithelia are involved in metabolism, excretion, respiration, and ionic regulation. [7] These two layers of epithelial cells are also responsible for all behavior in *Hydra*, generating motion of the polyp by exerting contractile force through myonemes, muscle processes that run longitudinally in the ectoderm, and

circumferentially in the endoderm. [8] Due to the perpendicular orientation of these processes, much of the literature assumes that they have opposing and mutually exclusive roles—an assumption that is tested by the techniques used herein.

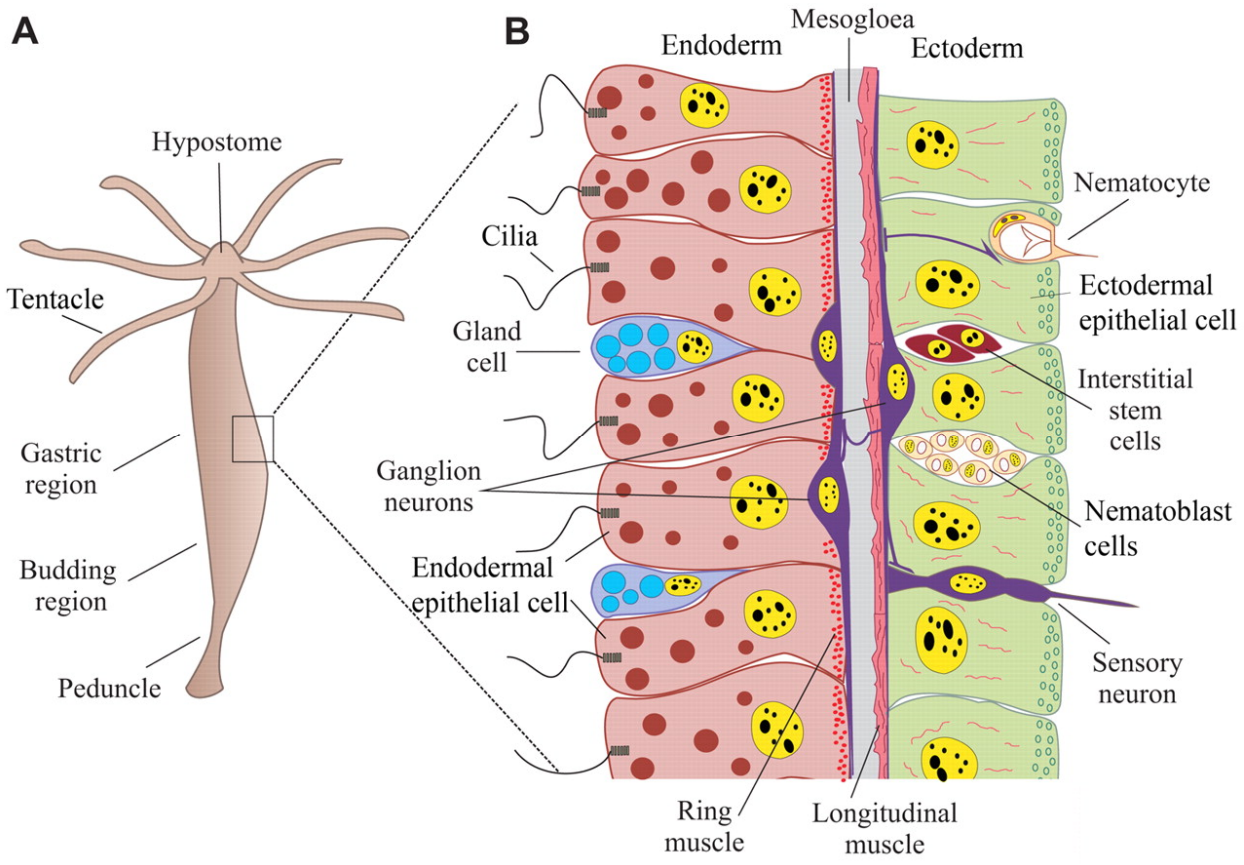

Figure 1: Anatomy of *Hydra*

A) Body plan of a *Hydra* polyp without buds or sexual differentiation.
B) A section of the two-layered body wall of *Hydra*. Reproduced from [9].

Muscle diversity in Metazoa, Cnidaria, and Hydra

Generally, muscle is a tissue in which calcium influx causes contraction based on the action of actin and myosin. Muscle types are best characterized in mammals, where they are broadly categorized as skeletal, cardiac, smooth, and myoepithelial. [10] Only skeletal and cardiac muscle are striated, meaning that the cells have visible stripes from repeating functional units called sarcomeres, in which rows of antiparallel actin and myosin are aligned and anchored to Z-disks. Skeletal muscles are connected to the skeleton and responsible for body motion, while cardiac muscle is specialized for pumping blood. Smooth muscle has irregularly organized bundles and sheets of cells, and is responsible for the contraction of hollow organs such as the gut as well as the vasculature. Myoepithelia are epithelial cells with muscle processes, and are found in glands such as the mammary and salivary gland. Bilaterian invertebrates also have striated and smooth muscle as well as myoepithelia that are implemented differently in their various body plans. [10] [11]

Cnidarian species, having completely different body plans and organization from bilaterians, of course show substantial differences in their muscle organization and usage. Epitheliomuscular cells are the dominant muscle type in all cnidarians, and in many cases are the only muscle type, as in the *Hydra* polyp. Typically, epithelial cells that also have muscular function are termed "myoepithelial" in bilaterians and "epitheliomuscular" in cnidarians. The epithelial myonemes form a continuous network of irregularly organized (smooth) actin filaments around the animal, and in hydrozoan polyps they are typically longitudinal in the ectoderm and circumferential in the endoderm, as in *Hydra*. In Hydrozoan species with a medusa (jellyfish) stage, medusae have a ring of circular striated muscle in the subumbrella composed of specialized epitheliomuscular

cells that are responsible for rhythmic contraction in swimming. This type of striated muscle is also found in other cnidarians, and phylogenetic evidence indicates that it evolved independently from the striated muscle in bilaterians, despite convergent morphology. [12] Other cnidarians also have non-epithelial myocytes embedded in their mesoglea that evolved independently of the specialized myocytes in bilaterians, but this is the exception to the rule of epitheliomuscular cells dominating cnidarian musculature (reviewed in [13]). Thus, the smooth epitheliomuscular cells of the *Hydra* polyp are quite representative of the dominant type of muscle tissue that is characteristic of Cnidaria, and the functional dynamics of which have been sparsely characterized, and never on a whole-system scale.

Figure 2: The Neuromuscular system of *Hydra*

Actin filaments are stained with phalloidin in red, and GFP-labeled neurons are green. Imaged by scanning confocal microscopy.

Neuromuscular anatomy, dynamics, and behavior in Hydra

Behavior

Since *Hydra* was first described by Antony Van Leeuwnhoek in 1702, [14] it has been observed that the polyp exhibits a variety of behaviors comprising individual motions such as elongation or bending of the body column, either spontaneously or in response to illumination, "nodding" or bending just below the tentacles [15] and contraction of individual tentacles or groups of them [16] or the entire body column. [17] These individual movements can be strung together into more complex compound behaviors such as the "contraction burst" that has been studied extensively, [17] [18] [19] and locomotor behaviors including somersaulting and inchworm motions [20] in which the polyp moves itself by first bending and elongating, then attaching its tentacles to the substrates, releasing its foot, contracting and reattaching its foot either beyond or near its tentacles. Another compound behavior is feeding behavior, induced by reduced glutathione from the ruptured cells of prey, that includes tentacle writhing, mouth opening, and sweeping of the tentacles toward the mouth to bring in captured prey. [21] [22] [23] [24] [25] Mouth opening has been characterized extensively, with evidence showing that it occurs through contraction of the ectodermal longitudinal muscles. [5] Recently, Shuting Han in the Yuste Lab has conducted a thorough analysis of *Hydra*'s behavioral dynamics, using machine learning tools to map the complete repertoire of behaviors, finding that the behavioral repertoire is quite stable to perturbation by stimuli, indicating that there may be a homeostatic mechanism involved in behavioral control. [3]

Neuromuscular anatomy of Hydra

The neuromuscular system underpinning behavior in *Hydra* has been studied through anatomical and electrophysiological methods for decades. The scale of the nervous system varies with the size of the animal, ranging from a few hundred to a few thousand cells. [26] Anatomically, neurons have been categorized into two types: sensory cells exposed to the external or gastric milieu [27] and ganglion cells that form the bulk of the lattice of cells known as the nerve net. [28] Evidence of synaptic connectivity in the neuromuscular system comes primarily from electron microscopy, with which both electrical and chemical synapses have been found throughout the body of *Hydra*. Electrical synapses are gap junctions composed of innexin monomers, and have been found between neurons, between neurons and epithelial cells, and between epithelial cells. [29] Eliminating some interneuronal gap junctions through treatment with an antibody for innexin-2 or blocking them all gap junctions with heptanol has been found to eliminate spontaneous contraction behavior. [30] In the epithelia, gap junctions are found between adjacent epithelial cells within both the ectoderm and endoderm, and also between cells in the ectoderm and endoderm at points where epithelial cells protrude through the mesoglea. [31] Chemical synapses mostly show dense-core vesicles, indicating a predominance of peptide transmitters, but small vesicles are also present. In addition to more typical polarized synapses, bidirectional synapses have been observed, with vesicles located adjacent to the synaptic membrane on both cells. [32] [33] [34] [35]

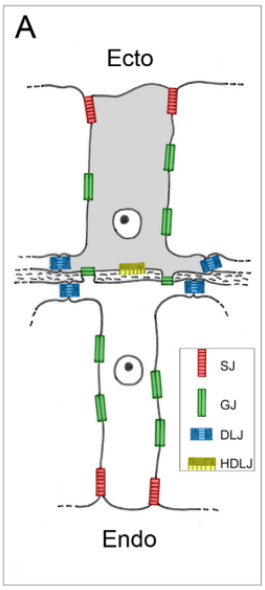

Figure 3: Gap junction connectivity between epitheliomuscular cells
Reproduced from **[31]**

Electrophysiology

Electrophysiological studies of *Hydra* were pioneered in a series of papers by Passano and McCullough [15], [36]–[38], who developed a technique for recording electrical activity in the polyp by attaching a relatively large microelectrode to the outside of the polyp by suction, recording the bulk potential from many cells extracellularly. Using this technique, it was found that the Hydra epithelia are excitable and able to propagate action potentials in the absence of neurons. [39] The technique revealed two main endogenous electrophysiological signatures in the body column of normal hydra—a large contraction pulse (CP) that occurs in conjunction with each longitudinal contraction of the polyp, which occurs in contraction bursts (CBs), [36] and smaller rhythmic pulses (RPs) that occur in the absence of any acute motion of the polyp. [37] These data suggest that CPs are large because they are composed of the combined electrical activity of neurons and epitheliomuscular cells, while RPs are much smaller potentials because

they only involve neurons, which are much smaller and mostly are buried beneath epithelial cells some distance from the recording suction electrode. Individual tentacle contraction has also been found to be accompanied by a pulse similar to a CP that is not propagated to the body column, termed a tentacle pulse (TP). [15] [16] Feeding behavior induced by glutathione has been found to inhibit CPs and TPs, but no positive electrical signature of mouth opening or tentacle bending was identified. [21] Recently, Christophe Dupre in the Yuste Lab has used calcium imaging with the genetically encoded calcium indicator GCaMP6s [40] to record the activity of all neurons in the polyp simultaneously. With this method, it was discovered that there are four sets of neurons in the polyp that do not overlap: the network which is associated with contraction bursts (CB), a small subtentacle network (STN) in the body column at the base of the hypostome, and two separate networks not associated with acute motion that correspond to the RPs observed electrically: RP1 in the ectoderm, and RP2 in the endoderm. Behavioral correlates of each neural set were found. CB neuron firing clearly occurs with every longitudinal contraction pulse of the polyp, and STN neurons fire when nearby patches of ecotoderm contract to effect nodding. Though there is no acute motion provoked by the firing of RP neurons, there is evidence that RP1 occurs more often during elongation, and RP2 prior to radial contraction, when the mouth opens to excrete gastric fluid. [2]

Voltage-gated channels

The variety of ion channels encoded in the *Hydra* genome has been explored using genomic approaches outlined below, but the channels are uncharacterized electrophysiologically and structurally, and the distribution of their relative expression in *Hydra* cells is unknown. The *Hydra* genome contains 35 different genes for voltage-gated potassium channels, [41] as well as

at least 7 genes for voltage-gated calcium channels. [42] Though voltage-gated sodium channel homologs are present in cnidarian genomes, [43] including that of Hydra, [42] and have a functional role in neuronal firing in some species, [44] [45] a study of sodium channel homologs from *Nematostella vectensis* shows that some actually preferentially conduct calcium, and that expression of true voltage-gated sodium channels is limited to certain neurons. The truly sodium selective voltage-gated channels that do exist in *Nematostella* appear to belong to a phylogenetic group unique to Cnidaria, indicating that sodium selectivity evolved independently in Cnidaria and Bilataria after these groups diverged. [46] Together, these data indicate that calcium-mediated action potentials play a foundational role in cnidarian cellular excitability. In the hydromedusan jellyfish *Aglantha digitale,* giant motor axons have been found to propagate separate sodium and calcium spikes independently, which stimulate fast and slow swimming movements, respectively. Sodium spikes have a larger amplitude and propagate at 1.4 m/s, while calcium spikes are smaller and propagate at 0.3 m/s. [47] The long duration of neural spikes recorded extracellularly in *Hydra* (93.0 ms full width at half maximum) [2] indicates that these spikes are likely to be mediated by calcium rather than sodium, as calcium spikes in *Aglantha* were similarly broad (40-60 ms) as compared to sodium spikes (1-2 ms). [47] The exclusive presence of action potentials based on calcium rather than sodium has been found in the nematode *Caenorhabditis elegans,* [48] and it is quite possible that *Hydra* operates with only calcium spikes as well, given that its small size and slow behavior may obviate the need for fast propagation of action potentials. Homologs of hyperpolarization-gated HCN channels have also been found in cnidarian genomes including *Hydra*, and their functionality was confirmed in the anthozoan *Nematostella vectensis*. [49]

Neurotransmission

Evidence regarding neurotransmission and neuromuscular transmission is quite sparse in *Hydra*. Some lines of evidence indicate that classical neurotransmission mediated by molecules including glutamate, GABA, glycine, and acetylcholine may occur, [50] but genes for receptors have not been identified, cloned or characterized. Initial analysis of the genome of *Hydra* showed the absence of genes coding for a vesicular acetylcholine transporter or acetylcholinesterase, [51] but two types of putative muscarinic acetylcholine receptor have been found, [52] and another study found a functional acetylcholinesterase in *Hydra* that is expressed in epithelial cells throughout the polyp, and not in neurons. [53] Evidence of peptide neurotransmission in *Hydra* however, is quite well developed. A large-scale peptide identification project conducted from 1993 to 2007 identified hundreds of peptides in *Hydra*, some of which were synthesized and tested for physiological effects. Antibody staining was conducted to identify localization patterns of some of the peptides—about half of them were found to be neuropeptides (expressed in neurons) and the other half epitheliopeptides (expressed in epithelial cells). Many of the epitheliopeptides were found to have effects on development. [54] Some neuropeptides were found to directly activate *Hydra*'s epithelial muscles, in some cases stimulating contraction of the body column [55] or tentacles, [54] and in other cases stimulating elongation. [56] [57] Receptors have been identified in *Hydra* that directly open ion channels upon peptide binding, one of the few examples of peptide-gated ion channels in nature. [58] These receptors were named HyNaC for *Hydra* Na^+ channel, but it was later found that they conduct all cations nonspecifically, so calcium could play a dominant role in their depolarizing currents. [59] There are genes for at least 12 different HyNaC subunits in *Hydra*, which can

assemble into at least 13 different ion channels with varying affinities for different *Hydra*-RFamide neuropeptides. The genes show different expression patterns in epithelial cells, including patches at the base of the tentacle, at the peduncle, and expression along the whole body column, as measured by *in situ* hybridization. (Fig. 3) [60] Other neuropeptides likely have a role in neurotransmission rather than neuromuscular transmission. It is likely that there are also GPCRs for peptides in *Hydra*—the genome contains hundreds of genes for GPCRs, several of which have homology with peptide GPCRs in higher organisms, but none have been cloned and characterized. [54] [61]

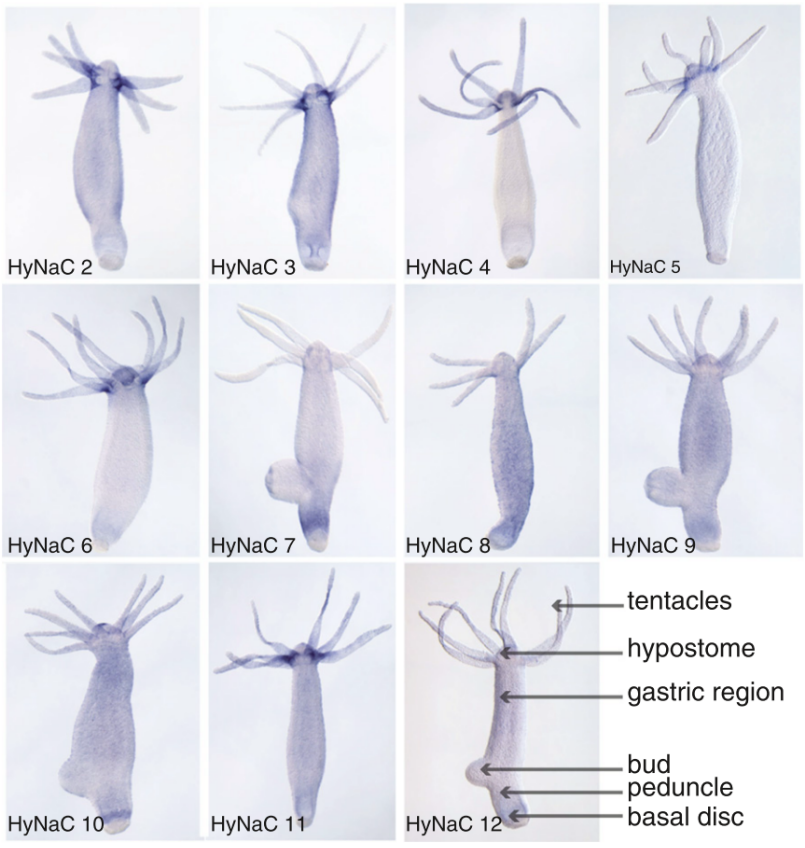

Figure 4: Distribution of expression of various HyNac Peptide-gated cation channels
Reproduced from [60]

The enteron: gastric cavity, hydrostatic skeleton, and osmoregulatory organ

The enteric region contained within the layered body wall of *Hydra* serves multiple purposes. It is the gastric cavity, wherein digestion occurs after prey is passed through the mouth during feeding behavior. Digestion occurs in this cavity in an at least partially extracellular process that involves initial lysis of prey cells by pore-forming proteins including Hydralysins [62] [63] and actinoporin-like toxins, [64] both of which are expressed by *Hydra* endodermal cells and integrate into the cellular membranes of prey, forming pores across the membrane. This causes osmotic lysis of prey cells despite the presence of a hard cuticle, and further disintegration and digestion of prey is thought to be accomplished with the aid of enzymes secreted by gland (zymogen) cells derived from the interstitial lineage that are located between endodermal epithelial cells. [65] [66]

Between feeding sessions, the enteric fluid serves as the hydrostatic skeleton of the *Hydra* polyp. As a soft-bodied creature, *Hydra* lacks the rigid tissues that serve as the skeletons of other animals, performing functions of force transmission that allow the contraction of muscles to elongate their antagonists and amplify the velocity, displacement, or force of muscle contraction. Like other soft-bodied animals, *Hydra* relies on a hydrostatic skeleton—an enclosed volume of aqueous solution that is not compressible. Thus, when the mouth is closed, the fixed volume of enteric fluid transmits forces from muscles to tissue motion. Longitudinal contractile force results in longitudinal contraction, while circular contractile force from the ring muscles of the endoderm results in longitudinal elongation. [67]

In addition to these functions, the enteric cavity plays in important role in osmoregulation, which may be critical to interpreting some results reported in this study. As a freshwater species that is

permeable to water and hypertonic to the medium it lives in, *Hydra* must constantly contend with an influx of water to its cells. Measurements of the ionic composition of fluids in *Hydra* tissue, enteric fluid, and external medium show that *Hydra* maintains an intracellular osmolarity more than 10 times greater than its medium, while enteric fluid is maintained at an osmolarity around half that of tissue. (Table 1) Potassium is notably enriched in tissue, while sodium comprises the majority of the ionic composition of the enteric fluid, which contains nearly no potassium [7], and is maintained at an electrical potential +25-40 mV relative to the medium external. [68] This indicates that potassium is transported into cells and sodium into the enteric fluid, likely due to action of the *Hydra* Na+/K+ ATPase ion exchange pump, [69] which is supported by the observation that the Na+/K+ ATPase inhibitor ouabain increases enteric potassium levels. [70] It is likely that that cation/chloride cotransporters are also involved, some of which could support the formation of fluid hypo-osmotic to cytosol by transporting water against its concentration gradient. Genes for such cotransporters have been cloned from *Hydra*. [71] The discovery of intercellular spaces in both ectodermal and endodermal epithelia that are connected to the gastric cavity by serpentine channels supports the idea that epithelial cells osmoregulate by secreting excess fluid into these spaces, pump ions and water between the spaces and cells to maintain membrane potential, retain potassium and expel sodium, and move the resulting hypo-osmotic fluid into the enteric cavity. [72] It was also found that increasing the osmolarity of the external medium reduces the frequency of *Hydra* contraction, [73] leading to the hypothesis that contraction has a role in osmoregulation, perhaps in expelling fluid from the enteron periodically. This possibility is complicated by the fact that the mouth opening is sealed shut by septate junctions when it is closed, [74] which is usually the case during contraction bursts. An

aboral pore does exist in the center of the basal disk, and has been shown to have permeability to dye, [75] but the permeability of this pore to fluids and ions has not been examined, nor has any variability or regulation of this permeability that could serve a function in osmregulation and regulating the volume of gastric fluid that serves as the hydrostatic skeleton. A different mechanism involving mouth opening is known to expel large volumes of fluid from the enteron periodically at a lower frequency than contraction bursts, [76] termed radial contraction in recent work from the Yuste lab. [2] This shows that radial contraction with mouth opening is the major means for the bulk release of gastric fluid, though more selective excretion may also occur through the mouth and/or aboral pore in the absence of visible opening. Longitudinal contraction bursts may have a role in this process, and additionally or alternatively serve to periodically move hypo-osmotic fluid from the intercellular exchange spaces to the enteron after ion and water exchange is complete. In either case, results reported below support the theory

TABLE 1—MEASURED OSMOLALITY AND ION CONCENTRATIONS OF TISSUE AND ENTERON FLUID OF *Hydra littoralis*

	Versene medium	Tissue	Enteron fluid
Osmolality (mOsm)	7–10/l.	120·6 (7) ± 4·2/kg	60·0 (17) ± 2·9/l.
Na^+ (mM)	1·7/l.	16·8 (11) ± 1·5/kg	46· 4(28) ± 1·9/l.
K^+ (mM)	0	50·9 (11) ± 4·7/kg	0·22 (29) ± 0·07/l.
Ca^{2+} (mM)	1·5/l.	—	—
Cl^- (mM)	3·0/l.	11·8 (12) ± 1·1/kg	6·5 (15) ± 0·8/l.
HCO^-_3 (mM)	1·2/l.	—	—
EDTA (mM)	0·12/l.	—	—

Composition of the outside medium (Versene) is also given. Number of determinations ± S.E.

that the main function of the contraction burst is osmoregulatory.

Table 1: Osmolarity of *Hydra* medium, tissue, and enteric fluid Reproduced from [7]

Studies of muscle on the system scale

In recent decades, the field of neuroscience has gained an appreciation that whole-system scale approaches are necessary to truly build understanding of the functional principles of nervous systems, as the single neuron may not be the relevant functional unit of these systems, and emergent properties likely play critical roles in how they work. [77] Muscular systems are similarly comprised of many parts that interact physically and through electrical and chemical signaling, but attempts to study them on a system scale have been sparse and largely limited to single organs. In vertebrates, cardiac muscle has been quite amenable to functional imaging, allowing for organ scale calcium and voltage imaging studies that have illuminated electromechanical function and system-level problems in wave propagation associated with disease mechanisms. [78] [79] Likewise, system-level approaches to the study of smooth muscle in the gut and oviduct including electrogastrography [80] and calcium imaging [81] [82] have been instrumental in uncovering functional principles of their operation. The mammalian musculoskeletal system is quite distributed spatially, so though functional imaging has found some utility in examining its parts for clinical purposes, [83] it is likely infeasible to record functional activity from the whole system at one, at least on the cellular scale. Calcium imaging has found utility in relating electrical and calcium dynamics in individual mammalian skeletal muscle fibers, [84] [85] and in elucidating the mechanisms of excitation-contraction coupling. In the nematode *C. elegans*, calcium imaging has been used to record activity transients in pharyngeal and vulval muscle and probe calcium channel function, as well as the unique form of excitation-contraction coupling in theses tissues. [86] [87] [88] Electrophysiology has revealed some functional principles of flight in the hawkmoth *Manduca sexta*, in which an EMG channel was recorded from the left and the right dorsolongitudinal wing muscle, and the two were

analyzed together to reveal the role of synergy between them. [89] Another study used calcium imaging to investigate power balancing in the ascynchronous indirect flight muscles of *Drosophila.* [90] Despite this proven utility, no attempt has been made to conduct calcium imaging of muscle on the scale of an entire animal, which may provide functional insight that would be obscured if only recording part of the system.

Hydra, being small, transparent, and amenable to transgenic approaches, [91] presents an ideal animal model for imaging the activity of the entire muscle system in an animal. It is known that the two layers of epitheliomuscular tissue are interconnected by gap junctions and innervated by a nerve net, and that they produce patterns of contraction that generate behavior, but many questions remain: What is the repertoire of these patterns of contraction? What groups of muscle cells are active in each of them, how large are they, and where in the animal are they located? How quickly do patterns turn on or off, and how do they change or propagate between cells? What mechanisms may be at play in excitation-contraction coupling in these tissues? In order to address these questions, calcium imaging was conducted in *Hydra* to record the activity of the muscle on a whole-system level, providing a view into the function of the sparsely understood epithelial muscles of a cnidarian.

RESULTS

Imaging the complete muscle activity of Hydra

To perform simultaneous calcium imaging in both the ectodermal and endodermal epitheliomuscular cells of Hydra, I used two different genetically encoded fluorescent calcium indicators with different spectral properties. GCaMP6s is a widely used ultrasensitive fluorescent calcium indicator based on calmodulin and GFP, and as such it emits green light. [40] The other indicator I used is jRCaMP1b, one of a series of improved red-emitting calcium indicators that have been recently released. [92] The spectral separation of these indicators allows them to be excited and imaged simultaneously, with filters allowing for minimal bleedthrough between channels. Epithelial transgenic lines were generated by modifying a plasmid designed by Dr. Rob Steele to express GFP under a *Hydra* actin promoter. (Addgene #34789). [93] For our purposes, the coding sequence for GFP was replaced by either GCaMP6s or jRCaMP1b, both of which were codon optimized for *Hydra* to account for its extreme A/T bias in codon distribution. The resulting plasmids were then injected into fertilized *Hydra* eggs using the typical protocol for making transgenics. [94]

Hatched *Hydra* were screened for expression, which can occur in any of the three stem cell lineages: ectoderm, endoderm, or interstitial, or a combination. For this study, polyps expressing GCaMP6s in ectoderm, endoderm and interstitial lineage were isolated, as was a polyp expressing jRCaMP1b in the endoderm. These polyps were fed, and buds were screened for expression of the transgene, keeping the buds with highest labeling percentage as the populations expanded. A line expressing GCaMP6s in nearly every interstitial cell was used in a previous study of the nervous system. [2] In epithelial transgenic lines, unlabeled cells are obviously

visible as dark holes in an otherwise fluorescent sheet of cells, allowing for the definitive selection of polyps with a clonal population of transgenic epithelial cells. To combine labeling from both indicators in a single line of polyps, we utilized grafting, a classic technique in the study of Hydra for combining tissue from multiple polyps. [95] In our case, the oral half of a polyp expressing jRCaMP1b in the endoderm was grafted to the aboral half of a polyp expressing GCaMP6s according to an established procedure. [R. Steele, personal communication] The resulting chimeric animal was fed regularly, leading to differential tissue displacement between the ectoderm and endoderm as the cells divided, and resulting in areas of body wall containing both transgenic endoderm and ectoderm. Buds were collected and screened until a polyp was found that had nearly complete labeling in both endoderm and ectoderm. Unlabeled cells were occasionally found in the ectoderm in further imaging due to unknown processes, but they did not interfere with data collection. The same procedure was used to create *Hydra* expressing jRCaMP1b in endodermal cells and GCaMP6s in neurons.

Imaging was performed by mounting polyps between two pieces of coverglass using a spacer with a thickness of either 100 or 200 μm (depending on animal size) to constrain the animal to a plane, within which it can move freely. Single color imaging experiments were performed with a fluorescence dissection microscope. To image signal from both GCaMP6s and jRCaMP1b simultaneously, a spinning disk confocal system was used that excites each fluorophore with a laser (488 nm and 561 nm, respectively) and splits the emission light with a dichroic mirror, sending green light to one camera and red light to another. Cameras were aligned with a grid, and the small amount of bleedthrough from the long-wavelength tail of GCaMP6s emission into the red channel and was measured as a percentage of GCaMP channel. This percentage of each

image from the green channel was then subtracted from the corresponding red image which had been collected simultaneously. Recording was done at 4x or 10x magnification, with a framerate from 3-10 frames per second depending on the experiment.

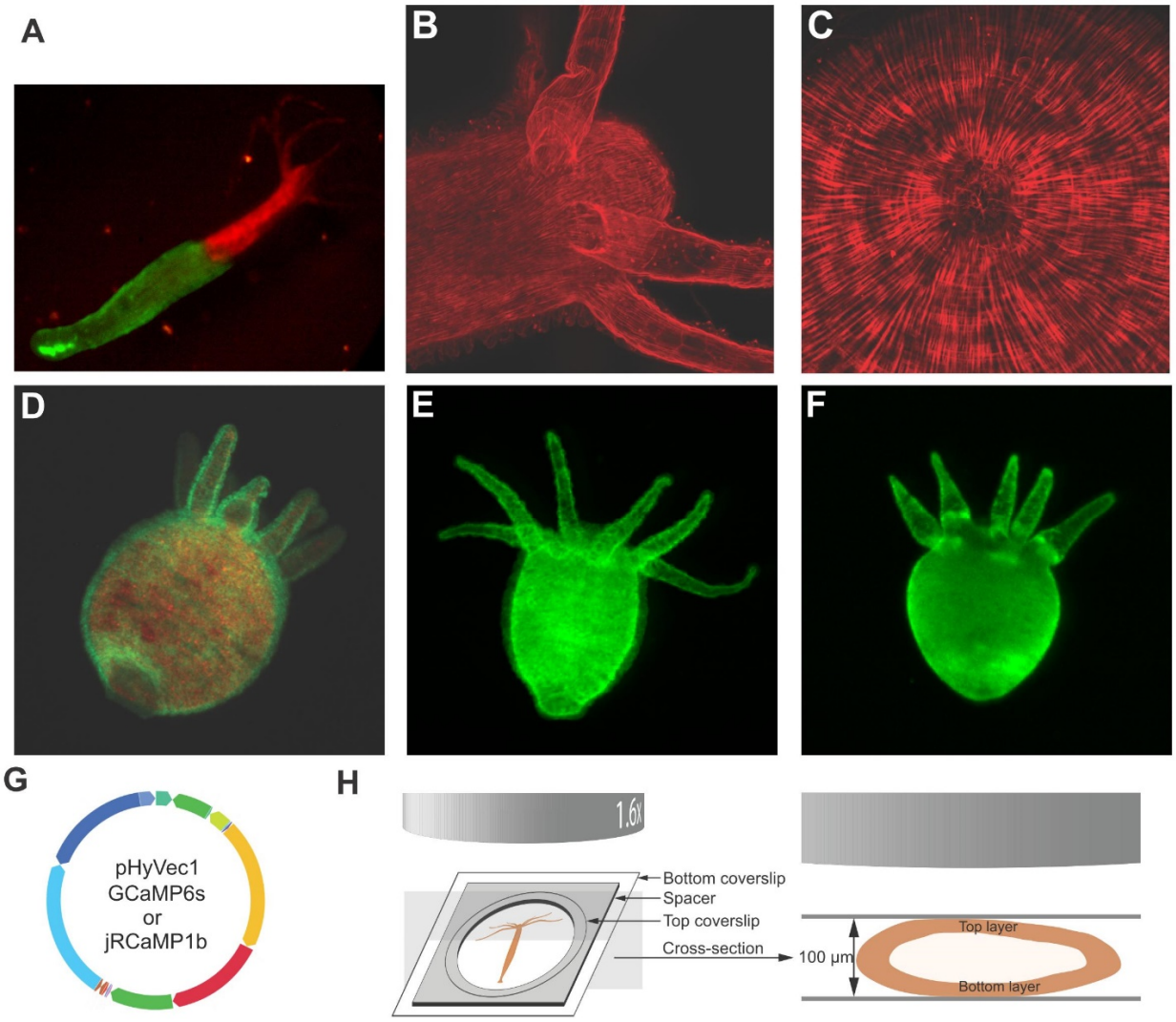

Figure 5: Transgenics and imaging

A) Grafted polyp expressing jRCaMP1b in oral endoderm and GCaMP6s in aboral ectoderm
B) Phalloidin-TRITC staining, lateral view showing longitudinal ectodermal myonemes
C) Phalloidin-TRITC staining, view of hypostome with closed mouth at center showing longitudinal ectodermal myonemes radiating from mouth and circular endodermal myonemes
D) Polyp expressing jRCaMP1b in the entire endoderm and GCaMP6s in the entire ectoderm
E) GCaMP6s expression in ectoderm only
F) GCaMP6s expression in endoderm only
G) Plasmids used for transgenics
H) Imaging preparation

Diversity of patterns of epithelial calcium activity

Whole-muscle imaging of Hydra reveals a diversity of activity patterns underlying the motion of the polyp that generates its behavior. Extensive observation made it clear that calcium activity patterns fall into a number of categories based on extent of activity (percentage of each epithelium involved), location of activity, dynamics of activity, and whether activity propagates between cells or activates many cells nearly simultaneously. In this section, I present a survey of the types of activity observed, including the characteristics that separate it from the other types and any surprising results observed. The data illustrating the various patterns are presented in Fig. 6, with a subpanel for each type of activity pattern. The left part of each subpanel shows the key frames of the activity pattern to illustrate the motion and calcium dynamics involved. The upper panels show fluorescence from jRCaMP1b in the endoderm, and the lower panels show fluorescence from GCaMP6s in the ectoderm. The right part of each subpanel shows a kymograph of calcium activity over time for each fluorophore. Each column in the kymograph represents a maximum projection of the rows of a frame from the fluorescence movie, with a heat map representing higher fluorescence values with warmer colors. Thus, both polyp motion and fluorescence are visible in the kymograph, allowing for the comparison of epithelial calcium activity with motion.

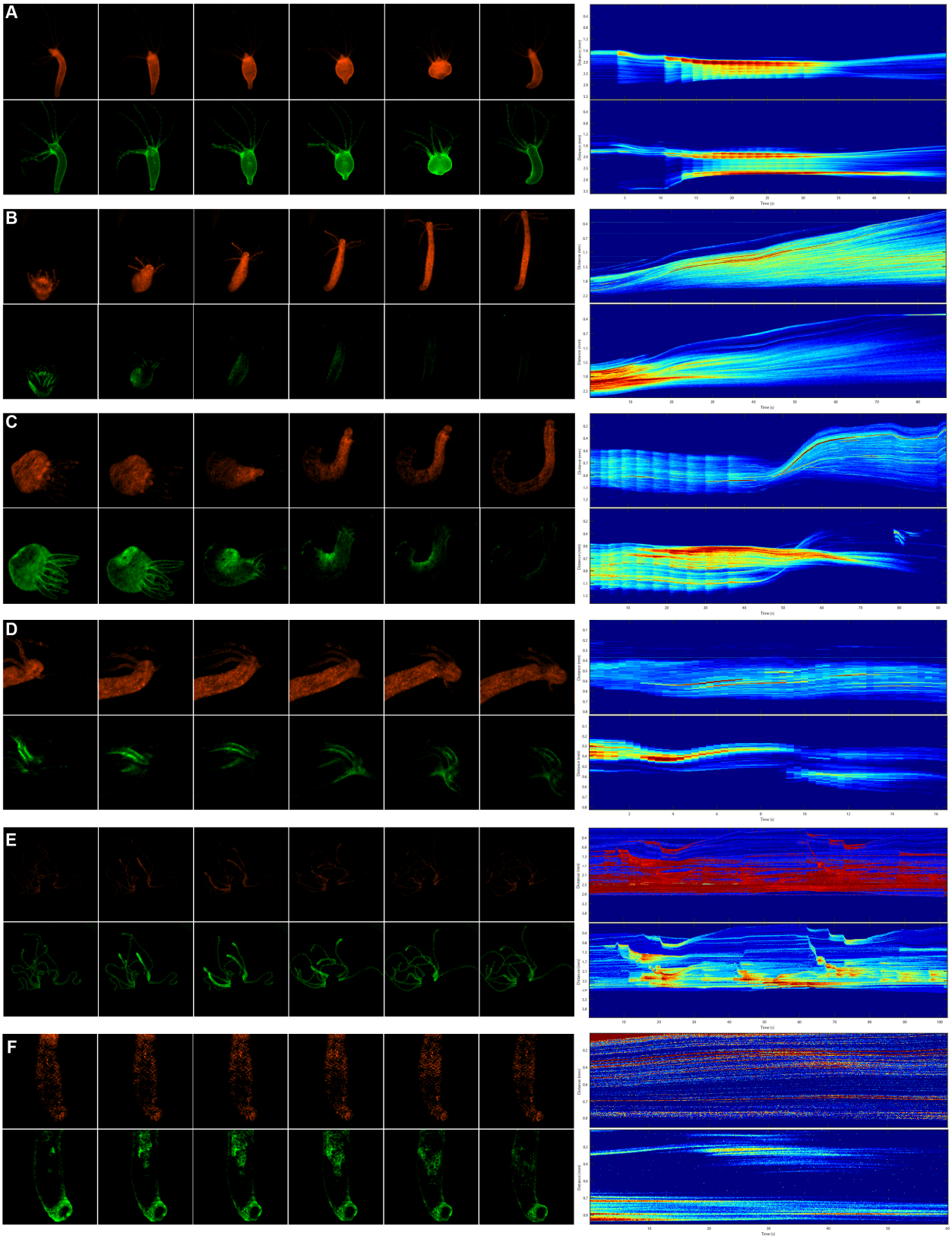
A
B
C
D
E
F

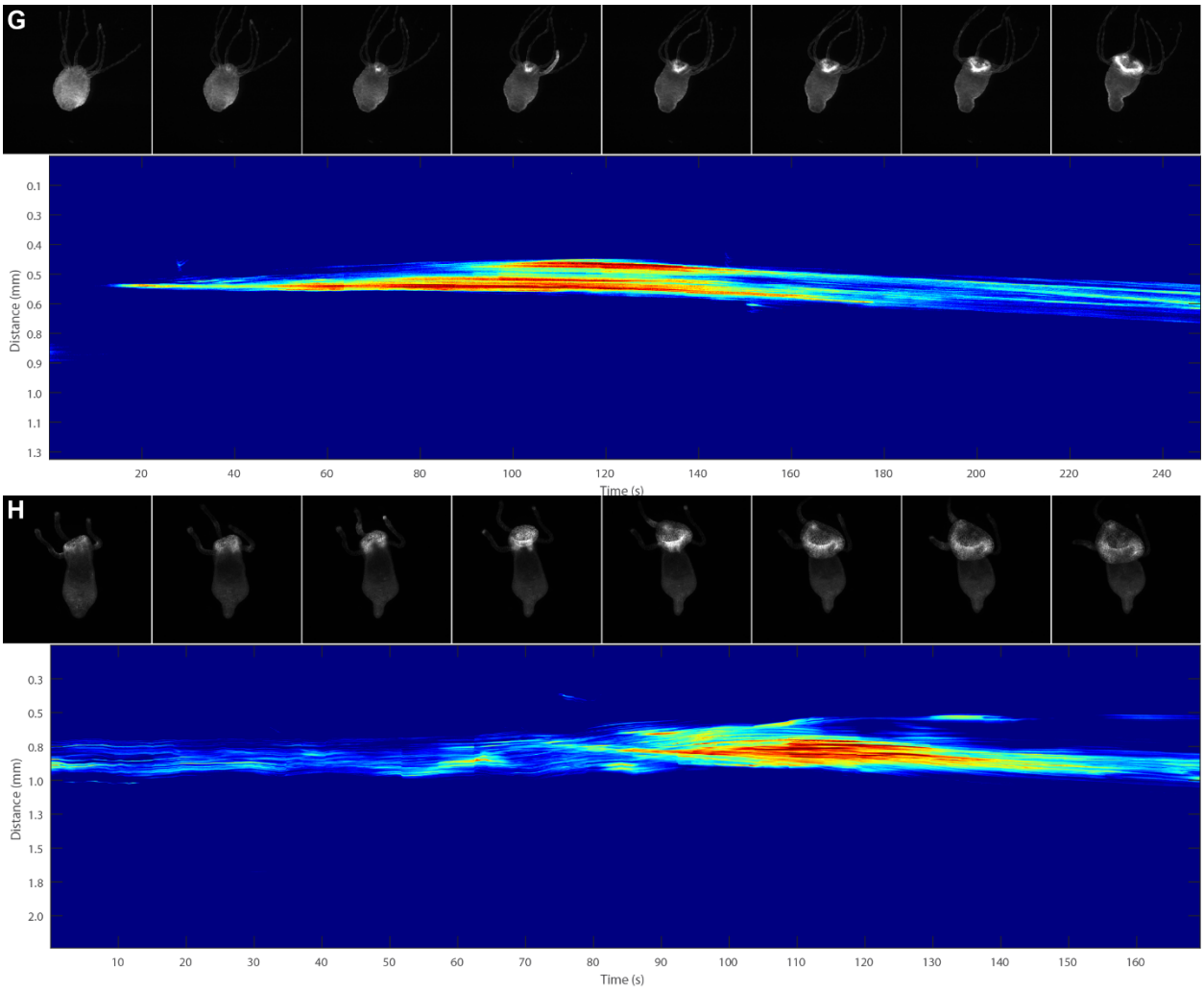

Figure 6: Survey of patterns of epithelial activity

All panels show key frames of an identified muscle pattern (left) and kymographs of activity over time (right) for both endoderm (top) and ectoderm (bottom)

A) Longitudinal contraction burst
B) Elongation
C) Bending
D) Nodding
E) Tentacle contraction
F) Slow wave, body column
G) Mouth opening, ectoderm
H) Mouth opening, endoderm

Contraction bursts

The most dramatic motion the Hydra polyp makes is a full-polyp contraction. This usually occurs as part of a contraction burst, during which many individual contraction pulses occur, and the characteristics of this behavior have been studied extensively. [17] In all previous literature, it has been assumed that longitudinal contraction pulses only involve activity in the ectodermal muscle, since it contracts longitudinally. Surprisingly, calcium imaging reveals that both ectoderm and endoderm are activated during longitudinal contraction pulses, with all cells in both epithelia showing rapid calcium influx with near simultaneity, as is visible in the vertical lines in both endodermal and ectodermal kymographs in Fig. 6A, reflecting rapid calcium activity across both epithelia accompanying each individual contraction pulse within the burst. To eliminate the possibility that increases in fluorescence observed in kymographs were due to the concentration of fluorescent protein upon contraction of tissue, the same experiment was performed using a polyp bearing the calcium-insensitive fluorescent proteins EGFP and dsRed in the endoderm and ectoderm, with showed no fluorescence dynamics. (Appendix, Fig. B) Additionally, mean fluorescence traces were calculated from every pixel in each frame, thus keeping the total amount of sampled tissue constant, avoid any artifacts from tissue compression. In these traces, it is clear that the measured signal reflects calcium dynamics, with peaks occurring in both ectoderm and endoderm during each contraction pulse. (Fig. 7) The cross-correlation between the first derivative of the smoothed signal from the two channels peaks at [0.97] at a lag of zero frames, indicating true simultaneity of epithelial activation on this timescale. (Fig. 7B) To characterize the initiation kinetics of contraction pulses, pulse traces from the ectoderm and endoderm were aligned based on their pre-pulse minima and averaged.

The mean trace and standard error of the mean were plotted for each tissue, along with the first derivative of the endodermal trace, calculated as the difference between samples of the mean trace. (Fig. 7C) The derivative shows a clear peak at 0.15 seconds after pulse initiation, indicating the latency from pulse initiation to peak calcium influx. The ectoderm showed identical kinetics and was omitted for graphical clarity. In further sections below, the contraction burst is further analyzed to reveal the relationship of calcium levels with tissue motion and to assess the fine dynamics of initiation of contraction pulses.

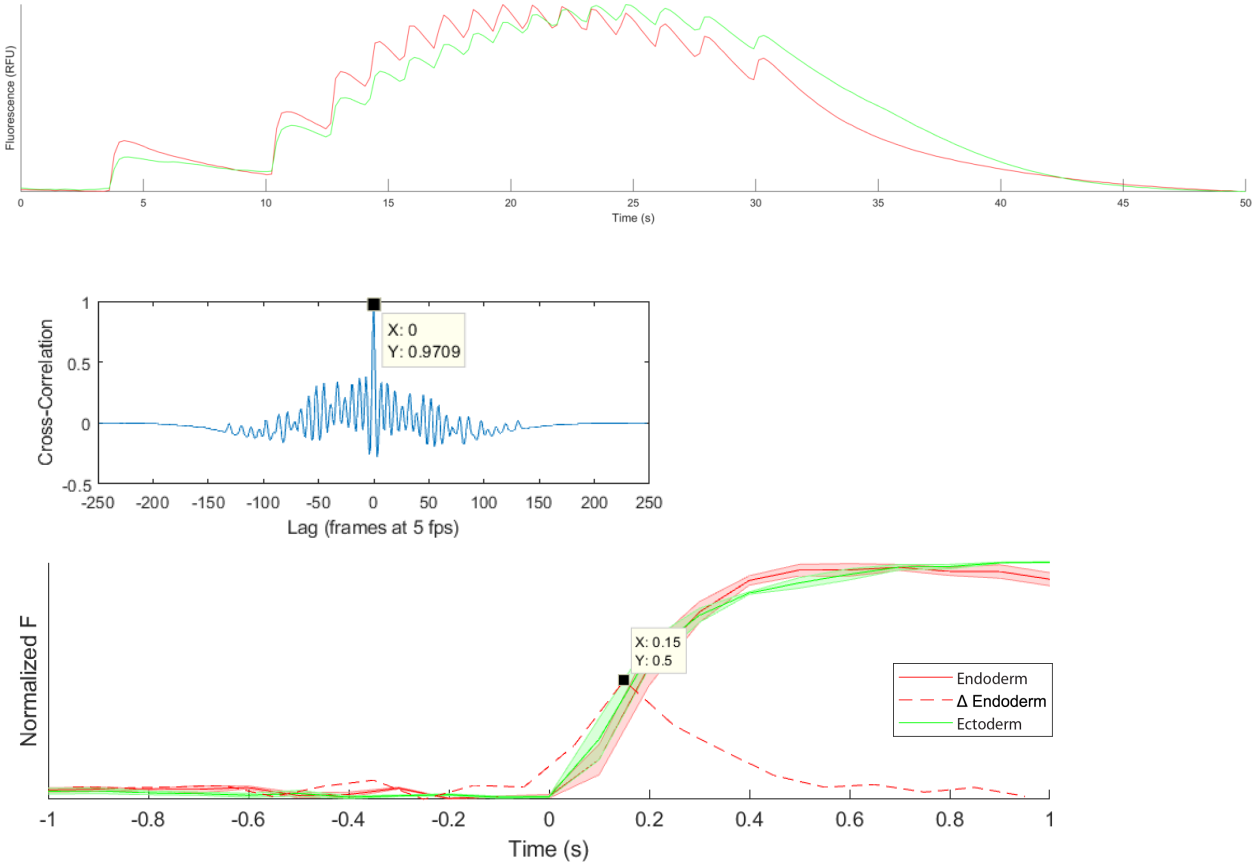

Figure 7: Fluorescence traces during contraction bursts

a) Fluorescence traces showing mean frame fluorescence of jRCaMP1b in endoderm (red) and GCaMP in ectoderm (green) during a contraction burst
b) Cross-correlation of first derivative of smoothed signals peaks at lag = 0

c) Contraction pulse initiation kinetics. Mean of n=3 traces plotted for each tissue, along with the S.E.M. (shaded regions) and derivative of endodermal trace indicating latency from initiation to peak calcium influx. Ectodermal trace showed an identical latency and was omitted for graphical clarity.

Column elongation

After each contraction burst, the Hydra polyp passively relaxes into its typical posture, with calcium levels decreasing in both epithelia as this occurs. (Visible in Fig. 7) The relaxed posture of Hydra, at which elastic forces from compression of tissues are minimized, can be assessed by treating live Hydra with relaxant agents including Chloretone (also known as chlorobutanol) and linalool (R. Steele, personal communication), and is depicted in Fig. 3, where a polyp has been fixed after being relaxed with linalool. The polyp can also elongate actively to become longer than it is when relaxed. In agreement with previous assumptions, I find that this process involves calcium activity in the circular muscles of the endoderm, which contract over a time course of tens to hundreds of seconds to exert force on the hydrostatic skeleton, elongating the tissue. A gradual increase in calcium levels exclusive to the endoderm is visible both in the kymograph (Fig. 6B) and in the whole-frame mean traces (Fig. 8) Measurement of latency from initiation to peak calcium influx indicates a delay of three seconds, indicating a slower mechanism is at play.

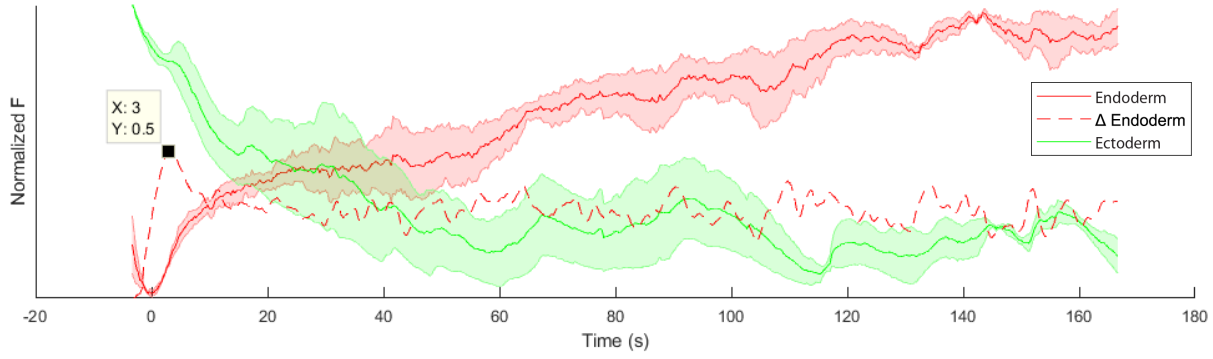

Figure 8: Mean fluorescence traces during active elongation

Fluorescence traces showing mean frame fluorescence of jRCaMP1b in endoderm (red) and GCaMP in ectoderm (green) during active elongation. N=3 traces were aligned to their pre-activation minima and averaged. Mean traces were plotted along with the S.E.M. (shaded regions). Derivative of the endodermal mean trace was calculated and plotted (dashed line), with the location of its peak indicating the latency from initiation of activity to peak calcium influx.

Bending

Another unique pattern of calcium activity consists of the radially asymmetrical activation of a growing patch of ectodermal cells in the peduncle and lower body column that causes the column to bend towards the contracting cells. This typically occurs after a contraction burst and before elongation, as has been observed previously as a component of a longer behavioral sequence involving either the sampling of a large area by the polyp by bending and elongating in various directions with the foot remaining attached to the substrate, or in locomotor somersaulting and inchworming behaviors in which bending and elongation is followed by tentacle attachment to substrate and movement of the foot. [96] In dual-epithelial calcium imaging, it is clear that the radially asymmetrical activity is exclusive to the ectoderm, (Kymograph 6C), while active elongation after bending involves slow endodermal activity as in elongation above. The ectodermal average trace is dominated by the initial contraction burst, but a clear increase in endodermal calcium is visible after the minimum reached after contraction. (Fig. 9) The ectodermal activity provoking bending begins at a location in the peduncle, and propagates between cells up the body column quite slowly, at a rate measured in another section below.

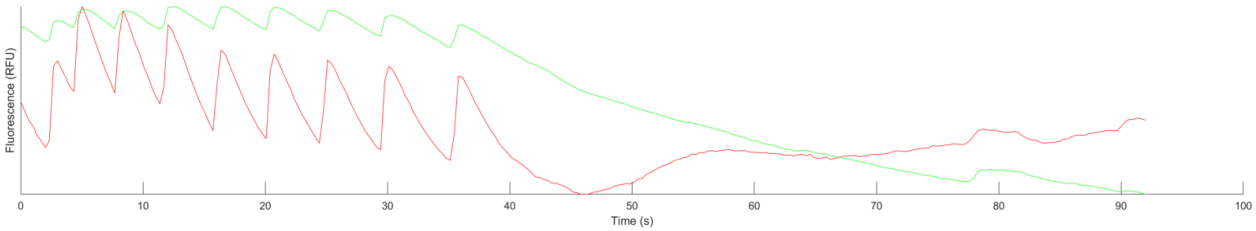

Figure 9: Mean fluorescence traces during bending

Fluorescence traces showing mean frame fluorescence of jRCaMP1b in endoderm (red) and GCaMP in ectoderm (green) during one example of bending

Nodding

A second form of radially asymmetric calcium activity is nodding, in which a small patch of ectodermal epithelium is activated in a region below the tentacles, causing the "head" of hydra (tentacles and hypostome) to move toward the activation. The radially asymmetric activity is exclusive to the ectoderm (Two consecutive examples occur in Kymograph 6D) but is accompanied by slow activity in the endoderm that causes elongation as part of the nodding motion. This is readily visible in the whole-frame mean traces (Fig. 10), in which the two bumps in GCaMP6s fluorescence correspond to the asymmetric contraction of patches of ectoderm, while the slow rise in jRCaMP1b accompanies active elongation via endodermal contraction.

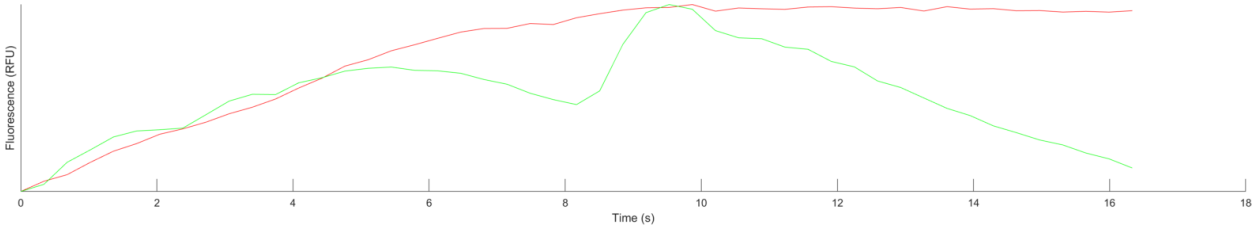

Figure 10: Mean fluorescence traces during nodding

Fluorescence traces showing mean frame fluorescence of jRCaMP1b in endoderm (red) and GCaMP in ectoderm (green) during nodding

Tentacle Contraction

Hydra tentacles contract individually and in groups, often in an increasing frequency leading up to a contraction burst of the whole body column that usually but not always includes the contraction of every tentacle. GCaMP6s and especially jRCaMP1b brightness is very low in the tentacles, so the signals are faint and noisy, but deletion of non-tentacle pixels in a movie allowed for the generation of Kymograph 6E, showing that both ectoderm and endoderm are activated during tentacle contraction, just as they are during longitudinal contraction of the body column. Lower expression levels may be due to a lower volume of cytoplasm or effects related to lower metabolism in tentacle cells. Mean whole frame traces are quite noisy, (Fig. 11a) but peaks of both traces occur together - the raw traces have a positive Pearson correlation coefficient of [0.300], which only increases to [0.303] with lowess smoothing of noise, but the correlation of the first derivative of these smoothed traces, related to calcium influx, increases to [0.589], indicating a true correlation of calcium influx.

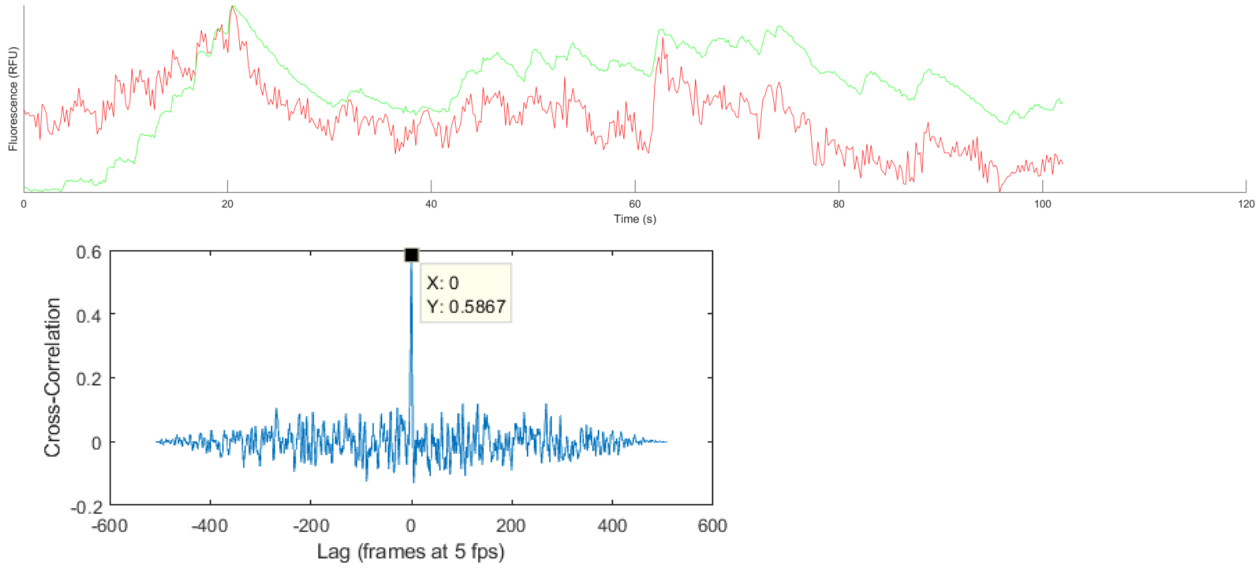

Figure 11: Mean fluorescence traces during tentacle contraction

a) Fluorescence traces showing mean frame fluorescence of jRCaMP1b in endoderm (red) and GCaMP in ectoderm (green) during tentacle contraction
b) Cross-correlation of first derivative of smoothed signals peaks at lag = 0

Slow wave

A rarer type of epithelial calcium activity involves a slow wave of activation that propagates down the body column from the oral end. This activity is radially asymmetric but only provokes subtle motion in the tissue. Figure 6F shows the progression of a slow wave that is prominent in GCaMP6s signal from ectodermal cells. The kymograph reveals apparently saltatory propagation as individual lines of activity appear in increasingly aboral positions over time. The velocity of propagation is consistent with diffusion of calcium and second messengers between cells rather than a propagated action potential, and is further analyzed below.

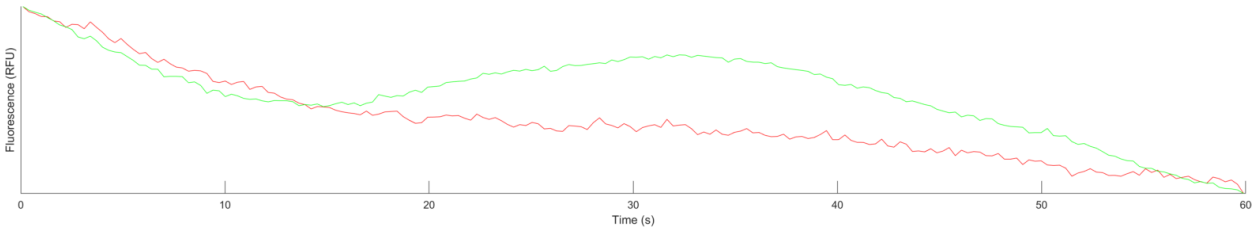

Figure 12: Mean fluorescence traces during body column slow wave

Fluorescence traces showing mean frame fluorescence of jRCaMP1b in endoderm (red) and GCaMP in ectoderm (green) during a slow wave in the body column

Mouth opening

Mouth opening is an active process in which septate junctions sealing the mouth shut are torn apart by muscle contraction in the tissue of the hypostome surrounding the mouth. It occurs as part of a feeding behavior that also includes kinking of the tentacles that is induced by reduced

glutathione either from freshly lysed prey cells or added exogenously by the experimenter. [97]

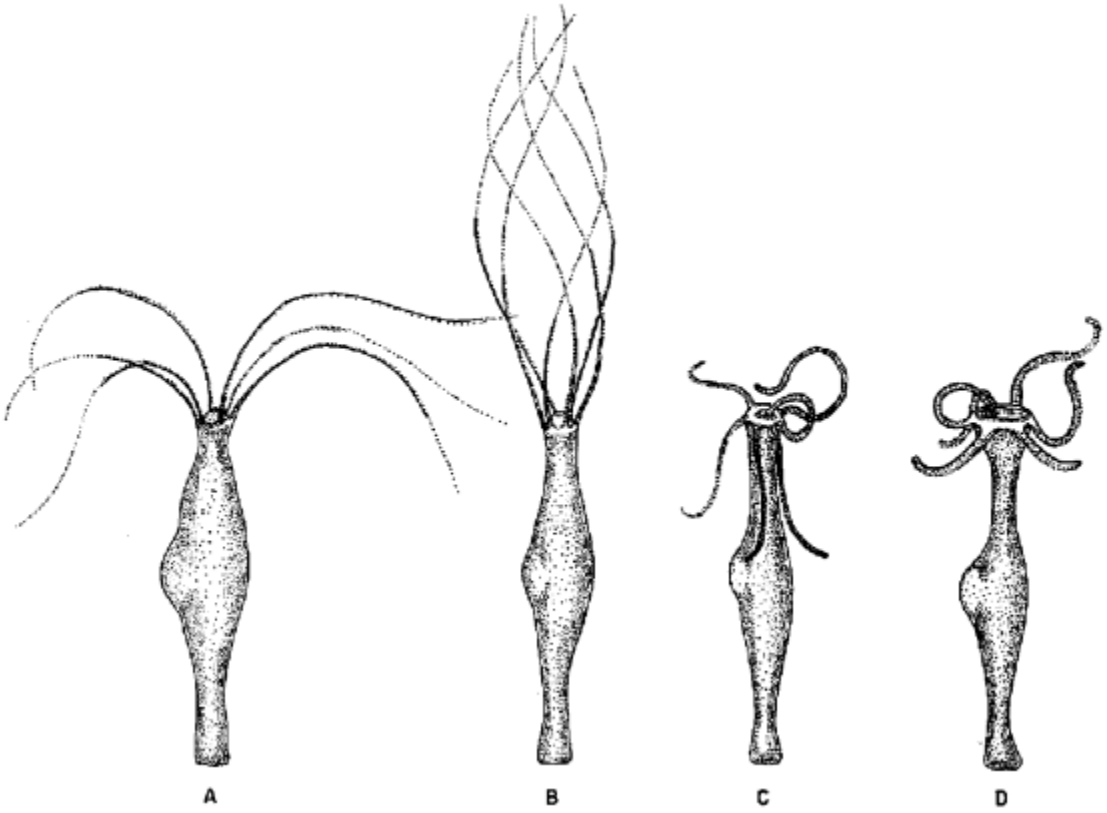

Figure 13: Stages of *Hydra* feeding behavior. Reproduced from [25]

A: Hydra in the absence of glutathione
B: Tentacles begin writhing and sweep inward toward the longitudinal axis
C: Tentacles bend toward the mouth and the mouth opens
D: Mouth is wide open and tentacles are in various stages of contraction

Calcium imaging using GCaMP6s separately in the ectoderm and endoderm during feeding behavior induced by 10 μM reduced glutathione has revealed that both of these tissues have calcium influx during mouth opening, and in both cases it starts at the tip of the hypostome near the mouth and propagates very slowly down the hypostome, past the tentacle attachment zone, and into the body column. (Kymographs 6G and 6H) The mouth is pulled open near the beginning of the process, when the slow wave of calcium activity is still localized to the perioral

area, and continues to open wider as the activity progresses. Mouth opening is often accompanied by a "writhing" motion of the tentacles in which multiple radially asymmetric portions of the endoderm and ectoderm are activated, often including most prominently an inner contraction halfway down the length of the tentacle that induces a "kink," bending the tentacle toward the mouth in a mechanism that brings paralyzed prey into the mouth for digestion

Relationship of motion with calcium influx in contraction bursts

To get a sense of the relationship between calcium activity and tissue motion in the Hydra polyp, a feature tracking approach was used to measure tissue motion in a dual-channel recording of epithelial calcium activity. Unique point features of the image were detected in the first frame using the minimum eigenvalue algorithm [98] and tracked between frames using the KLT point feature tracking algorithm. [99], [100] For each frame transition, the direction and velocity of feature motion was calculated. In Fig. 14A, the location of each feature is plotted on top of the fluorescence image using a marker with a hue corresponding to motion direction (according to

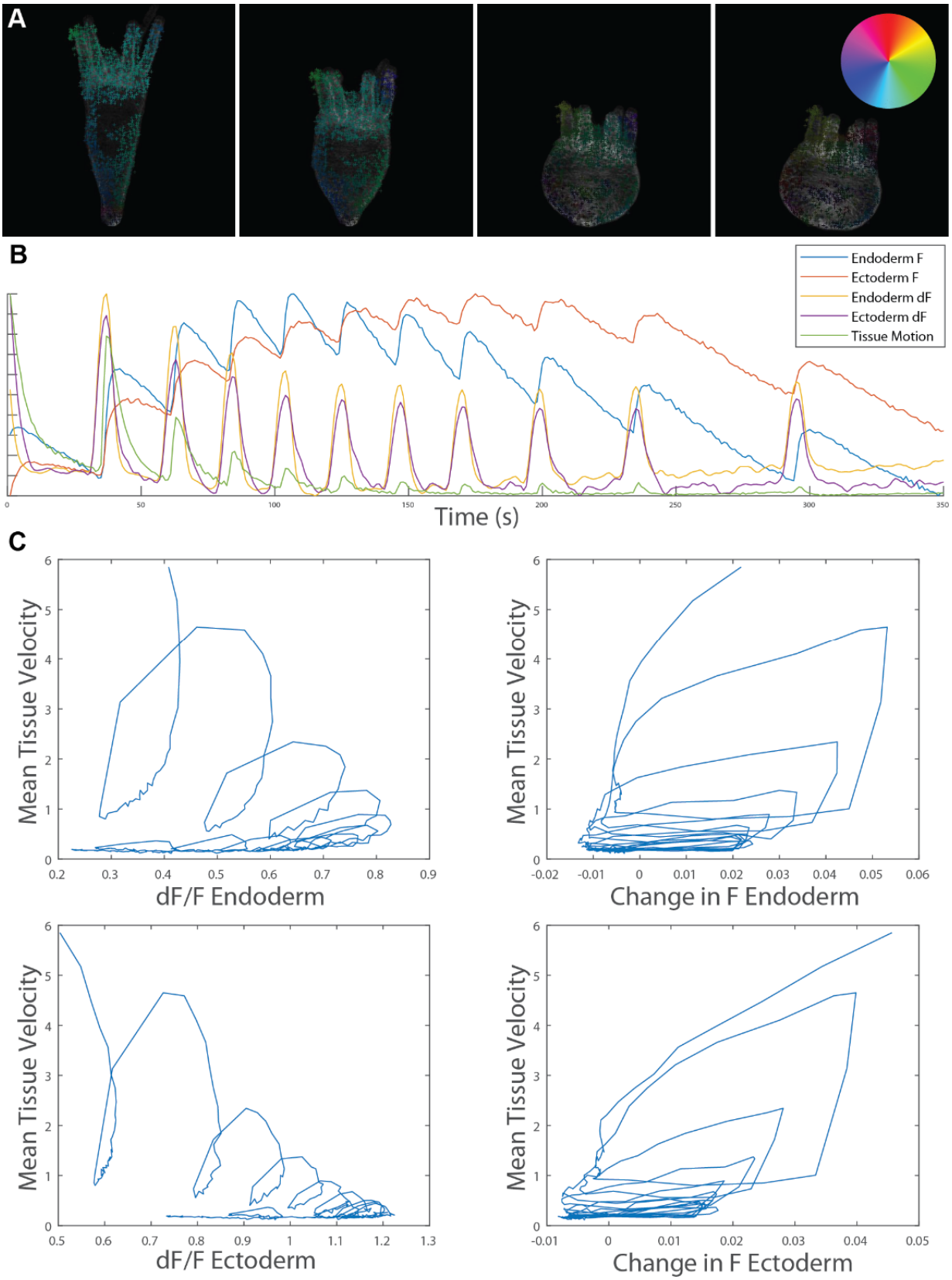
A
B
Endoderm F
Ectoderm F
Endoderm dF
Ectoderm dF
Tissue Motion
Time (s)
C
Mean Tissue Velocity
dF/F Endoderm
Change in F Endoderm
dF/F Ectoderm
Change in F Ectoderm

Figure 14: Relationship of motion with calcium influx

A) Features marked with a hue corresponding to direction of motion according to key, and saturation corresponding to velocity
B) Whole-frame mean fluorescence traces from endoderm and ectoderm, first derivative of each trace corresponding to calcium influx, and tissue motion velocity trace (mean velocity of feature motion)
C) Trajectories of fluorescence (left) and first derivative of fluorescence plotted against tissue velocity.

the key in the top right) and a saturation corresponding to motion velocity. A tissue motion velocity trace was generated by taking the mean of the velocity of each feature between each frame. In Fig. 14B fluorescence traces from both endoderm and ectoderm are plotted, as are the first derivatives of these traces and the mean tissue velocity trace. In this plot, it is clear that at the beginning of the contraction burst, the dynamics of calcium influx represented by the first derivative traces are more closely correlated with the motion trace than the raw traces are, but that the motion decreases over the course of the burst when the polyp is already contracted while the calcium influx decreases less. This indicates that the force being generated by calcium influx is likely balanced by the elastic forces of tissue deformation being exerted by the contracted tissue. Trajectories of dF/F and its first derivative versus tissue motion are plotted in 14D (starting at the top with maximal tissue velocity), where it is again clear that calcium influx (Change in F) is closer to being linearly related with motion than dF/F, but that there is a delay between the change in calcium influx and tissue motion. Delays were quantified by measuring the time from the beginning of calcium influx to the beginning of tissue motion, as measured by the peaks of the second time derivative of each of these traces. The mean delay between calcium influx and motion was thus found to be 0.35 seconds, with a 95% confidence interval of 0.0447

seconds. Peak motion nearly always occurred in the same frame as peak calcium influx, which always occurred before peak calcium concentration, at a quite variable interval of approximately 0.2-0.5 seconds.

Contraction burst initiation dynamics

As the kymograph analysis indicated that contraction pulses occur in the entire endodermal and ectodermal epithelia with near simultaneity, another approach was used to analyze the spatiotemporal dynamics of the initiation of these pulses with greater resolution in time. Recordings were made on the 2-color spinning disk confocal system at the maximum framerate of 55 frames per second, using a higher magnification 10x objective to increase signal. Contraction bursts were recorded using *Hydra* with dual epithelial labeling (n=2) as well as those with jRCaMP1b in endoderm and GCaMP6s in neurons (n=2). Portions of movies were collected where the polyp is at full contraction and largely stationary, thus obviating the need for tracking of regions of interest (ROIs) between frames. 47 contraction bursts were used from dual epithelial hydra, and 11 from neuromuscular. For dual-epithelial recordings, ROIs were defined at the oral and aboral ends and in the central body column directly between them. (Fig. 15A) For neuromuscular recordings, a single ROI was placed in the area containing endoderm and a large concentration of neurons in the peduncle. (Fig. 15C) Traces were extracted for each ROI, and processed by locally weighted scatterplot smoothing (Lowess). To compare the timing of calcium influx between the traces, the first derivative of each smoothed trace was computed and peaks were identified, corresponding to the times of maximum calcium influx. Peaks were compared between traces to identify relative timing between the traces (Fig. 15B, 15D). To plot

the relative timing of calcium activity in each trace, each ROI was compared to aboral endoderm, as this is the ROI that was measured in both dual-epithelial and neuromuscular comparisons.

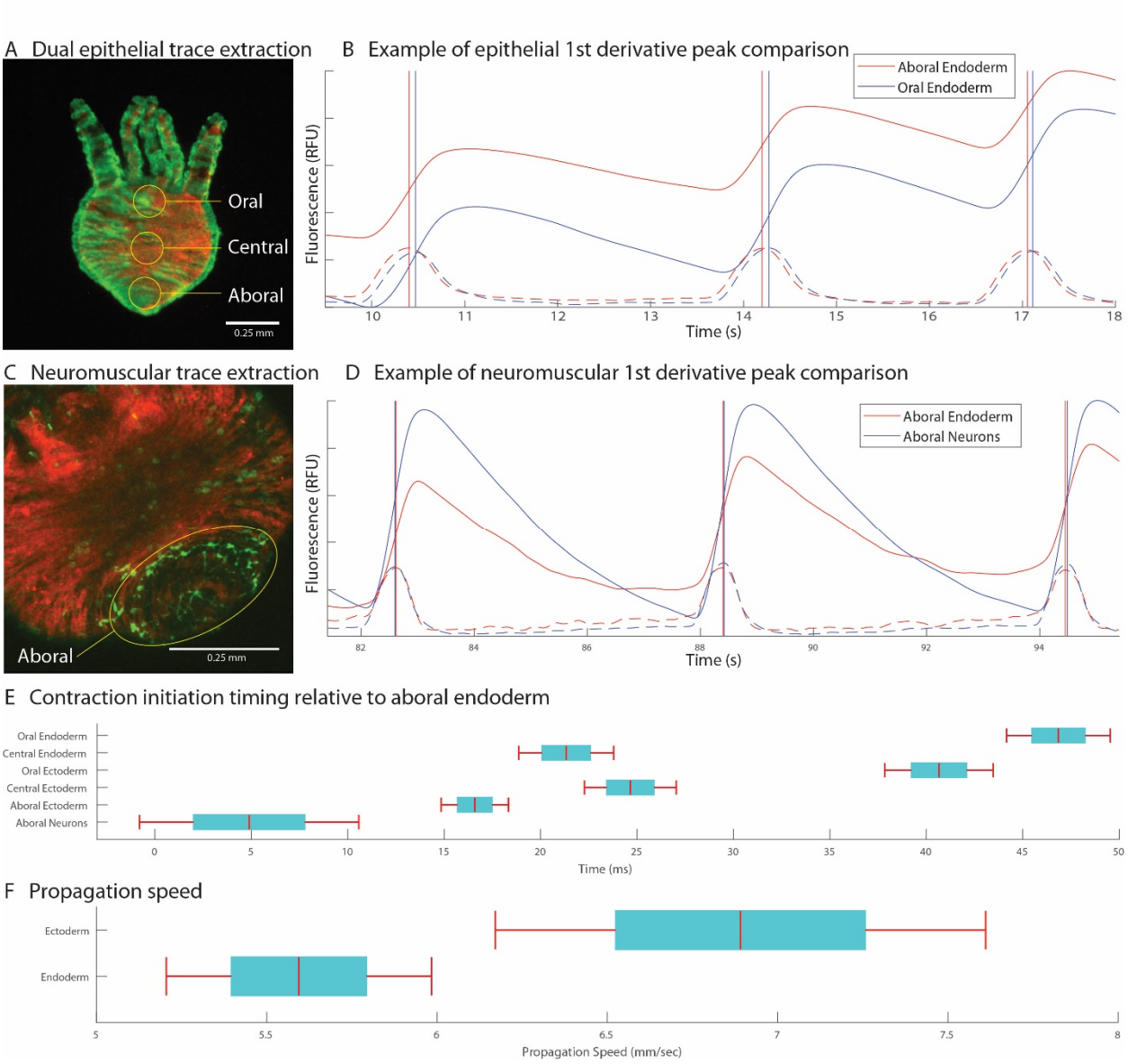

Figure 15: Contraction burst initiation dynamics

A) Regions of interest (ROIs) for dual epithelial recordings
B) Example of trace comparison between epithelial ROIs. Solid lines indicate smoothed fluorescence traces, dashed lines indicate their first time derivatives, and vertical lines indicate peaks in the first derivatives

C) ROIs for neuromuscular recordings
D) Example of trace comparison between neural and endodermal ROIs
E) Delays of each ROI relative to aboral endoderm. Central red line indicates mean, blue box indicates standard error of the mean, red whiskers indicate 95% confidence interval
F) Propagation speed from aboral to oral ROI measured in ectoderm and endoderm

Differences in kinetics between GCaMP6s and jRCaMP1b were corrected to properly align traces recorded with each indicated using an electrophysiological approach (See Appendix) Delays for each ROI versus aboral endoderm are plotted in Figure 15E, with bars centered on the mean showing the standard error of the mean and red whiskers showing the 95% confidence interval. These measurements show that all measured epithelial ROIs measure activation occurring after activation of the aboral endoderm. Central endoderm showed a mean delay of 21.33 ms, and oral endoderm a delay of 46.85, showing propagation of activation from aboral to oral endoderm at a mean velocity of 5.6 mm/s. Direct comparison between traces from jRCaMP1b and GCaMP6s would include artifacts arising from the different kinetics of these sensors, so the traces were aligned by calculating the timing of endodermal and ectodermal activation relative to each other, measuring each with GCaMP6s separately and comparing to an electrophysiological trace measured with a suction electrode on the peduncle (Appendix). This revealed a mean delay of 16.6 ms in the aboral ectoderm relative to the aboral endoderm, which was used to align the rest of the GCaMP6s traces with jRCaMP1b. Central ectoderm had a delay of 24.6 ms, and oral ectoderm 40.66, for a mean velocity of ectodermal conduction of 6.9 mm/s. Thus, aboral endoderm activates before aboral ectoderm in contraction pulses, but the pulses conduct toward the oral end faster in ectoderm, reaching aboral ectoderm roughly 6.2 ms before aboral endoderm. Neuromuscular comparisons were aligned assuming the same relative kinetics between indicators as in epithelial cells, and showed a mean delay of 4.9 ms in neurons versus aboral endoderm, though a delay of zero is inside the 95% confidence interval, so the assertion

that neurons activate after aboral endoderm does not reach significance. It may be the case that endoderm really does initiate contraction pulses, causing CB neurons to fire which then play a role in propagating the excitation to the ectoderm and the rest of the polyp, but this requires additional experiments to determine definitively—particularly useful would be suction electrode recording of CPs while also imaging calcium in neurons with GCaMP6s to be compared with similar recordings that have been performed with that indicator in endodermal epithelial cells.

Propagation velocity of slow waves

In the full survey of calcium activity patterns in the Hydra epithelia, three different patterns were discovered in which calcium activity propagates slowly between cells, forming a traveling wave of contraction: mouth opening, body column slow wave, and bending. Wavefront propagation within tissue over time was measured in all three cases, using a tissue feature as a landmark in cases of tissue motion. Velocities were calculated by fitting a line to the measured propagation as a whole, and in the case of mouth opening measured instantaneously between measurements to account for clear nonlinearity in propagation speed over the course of the process. (Fig. 16) The slope of the fitted line, representing average wavefront propagation speed, was found to be similar in mouth opening (2.6 microns/s) and body column slow wave (3.1 microns/s), though velocity opening in mouth opening changed considerable over the course of the process, beginning at 14.0 microns/s and ending at 1.3 microns/s. Wavefront propagation velocity in bending was quite linear, averaging 17.0 microns/s.

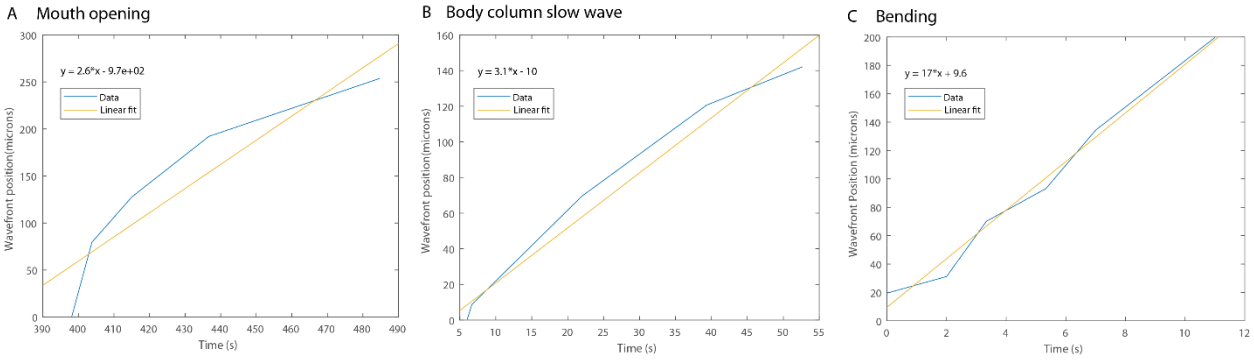

Figure 16: Wavefront propagation speed of slow waves in ectoderm

A. Wavefront propagation in ectoderm during mouth opening plotted as position over time. A line was fitted, with slope indicating average velocity of 2.6 microns/s. Instantaneous velocity is higher at the beginning of mouth opening (14 microns/s) than at the end (1.3 microns/s).

B. Wavefront propagation in ectoderm during body column slow wave plotted as position over time. Slope indicates average velocity of 3.1 microns/s
C. Wavefront propagation in ectoderm during bending plotted as position over time. Slope indicates average velocity 17 microns/s

DISCUSSION

Extensive cellular multifunctionality in Hydra muscular system

The epitheliomuscular cells that comprise the bulk of the Hydra polyp serve many functions—digestion, [101] formation of a protective exterior cuticle, [102] wound healing and regeneration, [103] innate immunity, [104] osmoregulation, [70] and muscle. [31], [105] Molecular evidence has further indicated that these cells show remarkable plasticity, taking on different characters when placed in different positions within the polyp tissue, presumably in response to secreted morphogens, and even upregulating neural genes when neurons are eliminated. [106] In this thesis, I have revealed that within the muscular function of the epitheliomuscular cells, there is further multifunctionality—the same cells participate in multiple types of calcium activity patterns with dramatically different characteristics to evoke different motions as part of different behaviors. Every epitheliomuscular cell participates in contraction pulses, with the entirety of both epithelia showing rapid calcium influx within 50 ms. Most of these cells also participate in other patterns that have different dynamics. For instance, cells in the endoderm of the body column can also participate in the slow activation leading to elongation. Cells in the ectoderm near the tentacle attachment zone can also be activated as part of a patch of neighboring cells in nodding, or in the slow waves of activity that occur during mouth opening or a radially asymmetric body column slow wave. Likewise, cells in the peduncle take part in the asymmetric activity of bending in addition to their role in contraction pules. The coexistence of these multiple types of activation in the same cells indicates that multiple distinct mechanisms are involved.

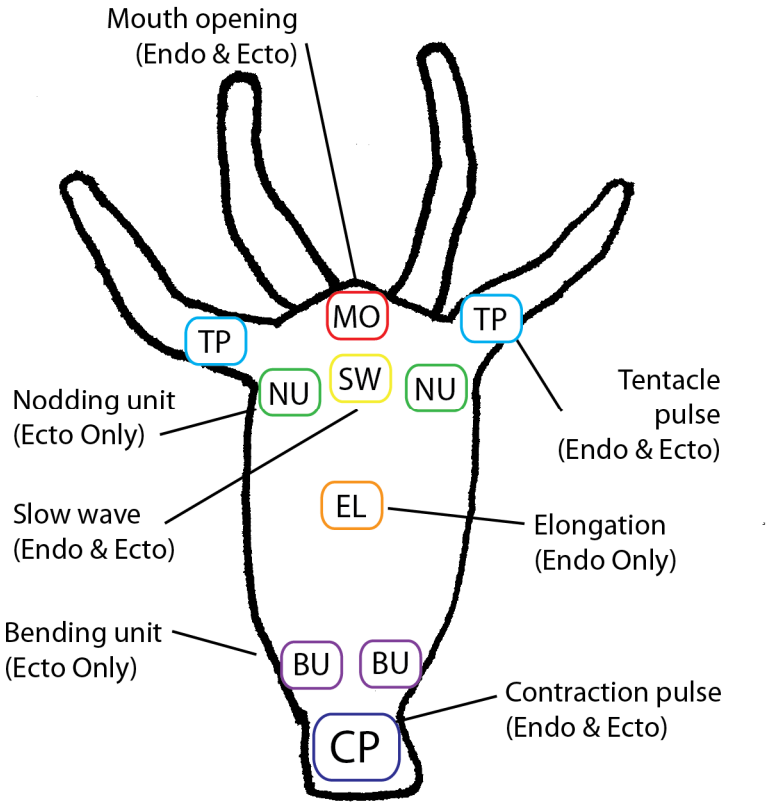

Figure 17: Identified muscle activity patterns in Hydra

Mechanisms of activity propagation across Metazoa

These experiments have identified patterns of epithelial calcium activity that have four fundamentally different types of dynamics.

1) Localized activity that is initiated quickly and does not propagate, which occurs in nodding when patches of ectoderm are activated below in the tentacle attachment zone, and in tentacle writhing in feeding behavior, when patches of cells in tentacles are activated. The rapid onset of this type of activity is consistent with the activation of ligand-gated calcium channels in the activated cells, which may evoke muscle contraction without causing enough depolarization to

yield an action potential that would activate cells outside the patch. A likely candidate for the type of receptor mediating this type of activity is a member of the HyNaC family or a similar peptide-gated cation channel, as iontotropic signaling is consistent with the relatively fast kinetics of activation observed, and some of these channels have expression patterns in the area in which nodding patches are visible. (Fig. 4 & 6D) Regardless of the type of channel involved, it is likely activated by a ligand secreted by the sub-tentacle network neurons identified in previous work from this lab to be associated with nodding. [2]

2) Global epithelial activity that propagates quickly between all cells or a large group of cells, such as the whole-polyp contraction pulses (CPs) that excite every epitheliomuscular cell in the polyp and the tentacle pulses (TPs) that excite every epithelial cell in an individual tentacle. Measurements in Fig. 15 show that calcium influx in CPs is initiated in the aboral epithelia and propagates to the rest of the body column at 5.5-7 mm/sec. This propagation speed is rapid relative to the slow waves described below, but slower than the propagation of CPs measured by electrophysiology with dual suction electrodes, where it was found that normal *Hydra* conduct electrically stimulated CP action potentials at 50 mm/sec, and nerve-free *Hydra* do so at 12 mm/sec. [107] This apparent contradiction could indicate that the propagating action potential involved in CPs stimulates calcium release from cellular internal stores or the opening of a different type of voltage-gated calcium channel, with the majority of calcium influx coming from this second mechanism. If propagation of calcium influx between cells depends on this secondary mechanism rather than just the action potential, any delays between the initial spike and secondary influx will be compounded as the wave propagates through the epithelia, accounting for the difference in propagation velocity measured electrophysiologically and via

calcium imaging. A similar situation has been found in gastric smooth muscle of mammals, in which gastric slow waves of contraction performing peristalsis are thought to propagate as voltage-accelerated calcium waves involving both an action potential and IP_3R-mediated Ca^{2+} release. [108]–[110] Another study found that in this tissue, spikes propagate at 48 mm/sec, while slow waves move at 13-18 mm/sec. [111] That these values are nearly identical to the propagation velocity of CPs measured electrophysiologically and by calcium imaging in Hydra indicates that similar mechanisms may be at play.

3) Slow calcium influx occurs globally in the endoderm during active elongation. The slow rise of calcium levels and diffuse nature of the activity throughout the endoderm indicates that it is likely to not be mediated by ion channels, but rather by the activation of G-protein coupled receptors (GPCRs), which have been shown to mediate the release of calcium from internal stores in cardiac muscle of mammals [112] [113] as well as vascular smooth muscle. [114] This is further supported by the observation that the only electrophysiological signature associated with active elongation in Hydra is the rhythmic pulse [115], which has been shown to originate from a set of neurons (RP1) that is associated with elongation but does not acutely provoke movement upon firing. [2] As such, these neurons likely release a neuropeptide or other transmitter that activates a G protein-coupled receptor expressed in endodermal epitheliomuscular cells that leads to a slow sustained rise in cytoplasmic calcium levels released from internal stores.

4) Epithelial activity that begins locally and propagates slowly between adjacent cells. This type of activity occurs in bending, mouth opening, and slow waves in the body column. In bending, the wavefront propagates at ~17 microns/sec, while in the other two it moves at ~3 microns/sec.

These speeds are consistent with a mechanism involving diffusion of a molecule between cells that mediates the release of calcium from internal stores in consecutive cells. Early experiments in squid axons demonstrated that calcium is quite immobile in cytoplasm [116] due to interactions with proteins, but the second messenger inositol triphosphate (IP_3) is known to be mobile in the cytoplasm and to mediate intercellular calcium waves in its diffusion through gap junctions. [117] This type of diffusion-based calcium wave is known to occur in the pancreatic islet, where they have been measured to propagate at a wide range of velocities ranging from 20-200 microns/sec, with a mean of 69 microns/sec [118] with a mechanism that depends on both IP_3 receptors and ryanodine receptors, which have distinct roles on releasing calcium from intracellular stores. [119], [120] Similar waves have also been found to take place in vascular smooth muscle [121] and in plant tissues [122].

Dual epithelial activation in contraction bursts and osmoregulation

In these studies, we were initially surprised to find that both ectoderm and endoderm show simultaneous calcium spikes during longitudinal contraction pulses, as these tissues have perpendicular myonemes and antagonistic roles in exerting force on the hydrostatic skeleton, so it was widely assumed that only ectodermal muscle, with its longitudinal myonemes, would contract during longitudinal contraction. The clear simultaneous contraction of both tissues indicates that ectodermal activation generates more force than endodermal activation, as the net effect is longitudinal contraction of the tissue. That circular contractile force is also generated during endodermal contraction is not likely to be an evolutionary accident, and can give us indication of the purpose of the contraction burst. Given that contraction burst frequency decreases when *Hydra* is placed in less hypotonic medium than its normal freshwater, [73] it is

likely that the force generated plays a role in osmoregulation. One likely function is to periodically contract epithelial tissue in such a way as to squeeze hypotonic fluid from extracellular spaces into the gastric cavity after ion exchange is complete. [72] It may also be possible that the physical pressure put on the gastric fluid during the contraction burst aids in expelling excess water without losing ions, moving water against its concentration gradient, perhaps in a mechanism involving aquaporin water channels, which have been found in the *Hydra* genome. [123]

CONCLUSION & FUTURE DIRECTIONS

Here I have presented the first survey of muscle system function on a whole-animal scale. Recording the calcium activity of the entire musculature of *Hydra* has allowed for the observation of the diversity of activity patterns that exist, and the identification of interesting features of these activity patterns that are readily apparent in the context of the entire system, but would be inaccessible via methods that record activity in single cells. In this view, it is clear that the single epitheliomuscular cell is not the relevant unit of function of the muscular system—cells are never activated individually, but only as a part of larger patterns that encompass groups of cells and can propagate between them. Through whole-animal calcium imaging, I was able to see how these patterns work within the system as a whole, characterize the extent of their diversity, and identify the four major types of contractile activity that coexist to compose them. Many individual epitheliomuscular cells exhibit more than one of these distinct types of activity, which operate by different mechanisms to expand the functional potential of these cells that are called upon to perform such a wide variety of roles in this anatomically simple polyp. The tissue specificity of genetically-encoded calcium sensors allowed us to spectrally dissect ectodermal

from endodermal activity, and assess the independent role of each tissue in each activity pattern. The surprising fact that both tissues fire during contraction pulses lends support to the decades-old theory that the function of these pulses is osmoregulatory, and identifies further questions as to whether this type of contraction serves to pump fluid into the gastric cavity, put pressure on gastric fluid to perhaps expel water against its concentration gradient, or both. Simply having an opportunity to watch the epithelial activity patterns on a whole-animal scale enabled us to map the function of the system as a whole, answered many questions, and posed many more. The simplicity of the body plan of *Hydra* indeed belies the functional complexity that is demanded of the cells that compose it in order to perform all of the functions that in higher animals are divided between many specialized cell types.

The musculature of *Hydra* exhibits a wide variety of functional activation patterns that have parallels to patterns that exist in tissues in vertebrates and even plants, revealing remarkable similarities given the at least ~750 million years that these organisms have been evolving independently. [1] The degree to which these mechanisms are conserved from a common ancestor or have been converged upon could tell an interesting story, and further analysis of the genes encoding the molecular components of muscle activation could illuminate this history—particularly the voltage-gated channels, GPCRs, IP_3 receptors, and ryanodine receptors.

Further functional studies of *Hydra* could also further elucidate the mechanisms indicated here by dynamics of calcium influx. Electrical recording in the subtentacle region could settle the question of whether activation of nodding patches of ectoderm involves an action potential or simply the non-propagating influx of calcium. Pharmacological dissection of calcium propagation mechanisms e.g. using blockers of intracellular calcium channels could help define

which types are involved in the putative voltage-accelerated calcium wave of the contraction pulse versus the slow influx from GPCR activation or the slow waves propagating by diffusion, though pharmacology can be difficult in *Hydra*, as most channels are so distantly related to bilaterian channels that familiar drugs used in other systems do not have the same effects in *Hydra*, or any effect at all. The role of these receptors could be assessed through the RNAi knockdown of their expression, or the deletion of the genes encoding them from the genome.

EXPERIMENTAL PROCEDURES

Hydra culture

Hydra polyps were kept in standard hydra medium in an 18° C incubator in the dark. [124] They were fed freshly hatched *Artemia* nauplii once a week for maintenance or more frequently to induce budding.

Transgenics and grafting

Transgenic lines were made using a plasmid based on pHyVec1 plasmid (Addgene cat#34789) [93], with EGFP replaced with either GCaMP6s or jRCaMP1b. In both cases the gene was codon-optimized for *Hydra* and synthesized. Standard embryo microinjection was performed [94] and chimeric transgenic hatchlings were isolated. Animals expressing GCaMP6s in the endoderm and ectoderm and jRCaMP in the endoderm were selected and budded, with buds bearing a higher percentage of labeled cells kept and propagated until the epithelia were clonally labelled. Endodermal jRCaMP was combined with ectodermal GCaMP6s by grafting, and again buds were selected to remove unlabeled cells.

Imaging and image processing

Imaging hardware

Imaging was done with a spinning disc confocal system (Solamere Yokogawa CSU-X1) with a camera for each channel (Stanford Photonics XR-MEGA10). Excitation light was from a 488 nm laser and a 561 nm laser. (Coherent OBIS) Whole polyp recordings used a 4x objective (Olympus UPlanSApom 4x/0.16), while higher magnification recordings used a 10x objective (UMPlanFl 10x/0.30 W) Single channel recordings were done on a Leica M165FC stereo fluorescence microscope with Hamamatsu ORCAflash4.0 sCMOS camera. Some dual channel recordings made use of a Hamamatsu W-VIEW Gemini system on this microscope.

Image processing

Background fluorescence was measured and subtracted from raw movies. The amount of bleedthrough from green to red channel was measured using a sample with only green fluorescence, and calculated as the percentage of green fluorescence visible in the red channel, which was 3.55%. Thus, this percentage of the green channel was subtracted from the red channel. Key frames were mapped to 8 bit using minimum and maximum threshold values to show relevant dynamics. Kymographs were calculated by finding for each frame the column of values corresponding to the maximum of each row in that frame.

Calculation of mean fluorescence traces

Calculation of mean fluorescence traces was performed by creating a binary mask to separate pixels measuring part of the polyp from those measuring background. A threshold for binarization was defined using a method based on Otsu's method [125] in which the threshold

defined by that method was divided by 10 to yield a threshold covering all pixels in the polyp and including minimal background. All pixels above the threshold were averaged for each trace. Traces were plotted either as change in fluorescence over minimum fluorescence (dF/F) or as relative fluorescence units (RFU), with each trace linearly scaled to have a minimum of zero and a maximum of one.

Simultaneous suction electrode recording and calcium imaging

Suction electrode recording was performed using a method based on the classic technique. [124] Glass electrodes were manually pulled from borosilicate glass with an outer diameter of 1 mm and inner diameter of 0.5 mm (Sutter Instrument) using a butane torch. Glass was bent to an angle of about 30 degrees toward one end to facilitate mounting, and heated and pulled to generate a thinned segment before being cut with a diamond scorer past the thinnest point to form an electrode visible in Fig. 18 A, B. The electrode was pointed in a micromanipulator and filled with *Hydra* medium, with a silver chloride wire in contact with the solution inside the electrode. The aboral end of a Hydra to be recorded was sucked into the electrode and suction was adjusted to keep the polyp in place without exerting undue force. Potentials between the electrode and a bath electrode were amplified with an AxoClamp 700B (Molecular Devices) in I=0 current clamp, and traces were recorded using PackIO, which can trigger recording of the electrophysiological data on a camera output signal [126] Calcium imaging was done simultaneously using excitation light from a mercury arc lamp filtered through a typical GFP filter cube, with a 4x objective (Olympus UPlanSApom NA = 0.16). Optical recording was done with a Hammamatsu ORCA Flash4.0 sCMOS camera recording at 100 fps.

REFERENCES

[1] E. Park, D.-S. Hwang, J.-S. Lee, J.-I. Song, T.-K. Seo, and Y.-J. Won, "Estimation of divergence times in cnidarian evolution based on mitochondrial protein-coding genes and the fossil record," *Mol. Phylogenet. Evol.*, vol. 62, no. 1, pp. 329–345, Jan. 2012.

[2] C. Dupre and R. Yuste, "Non-overlapping Neural Networks in Hydra vulgaris," *Curr. Biol.*, vol. 27, no. 8, pp. 1085–1097, Apr. 2017.

[3] S. Han, E. Taralova, C. Dupre, and R. Yuste, "Comprehensive machine learning analysis of Hydra behavior reveals a stable basal behavioral repertoire," *eLife*, vol. 7, Mar. 2018.

[4] M. P. Sarras, M. E. Madden, X. Zhang, S. Gunwar, J. K. Huff, and B. G. Hudson, "Extracellular matrix (mesoglea) of Hydra vulgaris: I. Isolation and characterization," *Dev. Biol.*, vol. 148, no. 2, pp. 481–494, Dec. 1991.

[5] J. A. Carter, C. Hyland, R. E. Steele, and E.-M. S. Collins, "Dynamics of Mouth Opening in Hydra," *Biophys. J.*, vol. 110, no. 5, p. 1191, Mar. 2016.

[6] H. R. Bode, "The interstitial cell lineage of hydra: a stem cell system that arose early in evolution," *J. Cell Sci.*, vol. 109, no. 6, pp. 1155–1164, Jun. 1996.

[7] D. J. Benos and R. D. Prusch, "Osmoregulation in fresh-waterHydra," *Comp. Biochem. Physiol. A Physiol.*, vol. 43, no. 1, pp. 165–171, Sep. 1972.

[8] J. J. Otto, "Orientation and behavior of epithelial cell muscle processes during Hydra budding," *J. Exp. Zool.*, vol. 202, no. 3, pp. 307–321, Dec. 1977.

[9] U. Technau and R. E. Steele, "Evolutionary crossroads in developmental biology: Cnidaria," *Development*, vol. 138, no. 8, pp. 1447–1458, Apr. 2011.

[10] B. Alberts *et al.*, *Molecular Biology of the Cell, Sixth Edition*. Garland Science, 2014.

[11] *The Evolution of Organ Systems*. Oxford, New York: Oxford University Press, 2007.

[12] P. R. H. Steinmetz *et al.*, "Independent evolution of striated muscles in cnidarians and bilaterians," *Nature*, vol. 487, no. 7406, pp. 231–234, Jul. 2012.

[13] L. Leclère and E. Röttinger, "Diversity of Cnidarian Muscles: Function, Anatomy, Development and Regeneration," *Front. Cell Dev. Biol.*, vol. 4, Jan. 2017.

[14] "IV. Part of a letter from Mr Antony van Leeuwenhoek, F. R. S. concerning green weeds growing in water, and some animalcula found about them." [Online]. Available: http://rstl.royalsocietypublishing.org/content/23/283/1304. [Accessed: 07-May-2018].

[15] L. M. Passano and C. B. Mccullough, "Pacemaker Hierarchies Controlling the Behaviour of Hydras," *Nature*, vol. 199, no. 4899, p. 1174, Sep. 1963.

[16] G. Kass-Simon, "Longitudinal conduction of contraction burst pulses from hypostomal excitation loci inHydra attenuata," *J. Comp. Physiol.*, vol. 80, no. 1, pp. 29–49, Mar. 1972.

[17] N. B. Rushforth, “Behavioral and electrophysiological studies of hydra. i. analysis of contraction pulse patterns,” *Biol. Bull.*, vol. 140, no. 2, pp. 255–273, Apr. 1971.

[18] R. H. Reis, “Spontaneous Change of Form of Pelmatohydra oligactis,” *Trans. Am. Microsc. Soc.*, vol. 63, no. 4, pp. 326–339, 1944.

[19] G. Wagner, “Memoirs: On Some Movements and Reactions of Hydra,” *J. Cell Sci.*, vol. s2-48, no. 192, pp. 585–622, Feb. 1905.

[20] A. Trembley, P. Lyonet, C. Pronk, and J. van der Schley, *Mémoires pour servir à l’histoire d’un genre de polypes d’eau douce, à bras en forme de cornes /*. A Leide : Chez Jean & Herman Verbeek, 1744.

[21] N. B. Rushforth and F. Hofman, “Behavioral and Electrophysiological Studies of Hydra. III. Components of Feeding Behavior,” *Biol. Bull.*, vol. 142, no. 1, pp. 110–131, 1972.

[22] E. E. Cliffe and S. G. Waley, “Effect of Analogues of Glutathione on the Feeding Reaction of Hydra,” *Nature*, vol. 182, no. 4638, pp. 804–805, Sep. 1958.

[23] W. Grosvenor, D. E. Rhoads, and G. Kass-Simon, “Chemoreceptive Control of Feeding Processes in Hydra,” *Chem. Senses*, vol. 21, no. 3, pp. 313–321, Jun. 1996.

[24] O. Koizumi, Y. Haraguchi, and A. Ohuchida, “Reaction chain in feeding behavior ofHydra: Different specificities of three feeding responses,” *J. Comp. Physiol.*, vol. 150, no. 1, pp. 99–105, Mar. 1983.

[25] H. M. Lenhoff, “Activation of the Feeding Reflex in Hydra littoralis,” *J. Gen. Physiol.*, vol. 45, no. 2, pp. 331–344, Nov. 1961.

[26] C. N. David, “A quantitative method for maceration of hydra tissue,” *Wilhelm Roux Arch. Für Entwicklungsmechanik Org.*, vol. 171, no. 4, pp. 259–268, Dec. 1973.

[27] J. A. Westfall, J. D. Wilson, R. A. Rogers, and J. C. Kinnamon, “Multifunctional features of a gastrodermal sensory cell in<Emphasis Type="Italic">Hydra</Emphasis>: three-dimensional study,” *J. Neurocytol.*, vol. 20, no. 4, pp. 251–261, Apr. 1991.

[28] C. J. P. Grimmelikhuijzen and J. A. Westfall, “The nervous systems of Cnidarians,” in *The Nervous Systems of Invertebrates: An Evolutionary and Comparative Approach*, Birkhäuser Basel, 1995, pp. 7–24.

[29] J. A. Westfall, J. C. Kinnamon, and D. E. Sims, “Neuro-epitheliomuscular cell and neuro-neuronal gap junctions inHydra,” *J. Neurocytol.*, vol. 9, no. 6, pp. 725–732, Dec. 1980.

[30] Y. Takaku *et al.*, “Innexin gap junctions in nerve cells coordinate spontaneous contractile behavior in Hydra polyps,” *Sci. Rep.*, vol. 4, Jan. 2014.

[31] A. Seybold, W. Salvenmoser, and B. Hobmayer, “Sequential development of apical-basal and planar polarities in aggregating epitheliomuscular cells of Hydra,” *Dev. Biol.*, vol. 412, no. 1, pp. 148–159, Apr. 2016.

[32] J. A. Westfall and J. C. Kinnamon, “Perioral synaptic connections and their possible role in the feeding behavior of Hydra,” *Tissue Cell*, vol. 16, no. 3, pp. 355–365, Jan. 1984.

[33] J. A. Westfall, S. Yamataka, and P. D. Enos, “ULTRASTRUCTURAL EVIDENCE OF POLARIZED SYNAPSES IN THE NERVE NET OF HYDRA,” *J. Cell Biol.*, vol. 51, no. 1, pp. 318–323, Oct. 1971.

[34] J. C. Kinnamon and J. A. Westfall, “Types of neurons and synaptic connections at hypostome-tentacle junctions in Hydra,” *J. Morphol.*, vol. 173, no. 1, pp. 119–128, Jul. 1982.

[35] J. A. Westfall, D. R. Argast, and J. C. Kinnamon, “Numbers, distribution, and types of neurons in the pedal disk of Hydra based on a serial reconstruction from transmission electron micrographs,” *J. Morphol.*, vol. 178, no. 2, pp. 95–103, 1983.

[36] L. M. Passano and C. B. McCULLOUGH, “Co-Ordinating Systems and Behaviour In Hydra: I. Pacemaker System of the Periodic Contractions,” *J. Exp. Biol.*, vol. 41, no. 3, pp. 643–664, Sep. 1964.

[37] L. M. Passano and C. B. McCULLOUGH, “Co-Ordinating Systems and Behaviour in Hydra II. The Rhythmic Potential System,” *J. Exp. Biol.*, vol. 42, no. 2, pp. 205–231, Apr. 1965.

[38] L. M. Passano and C. B. McCullough, “The Light Response and the Rhythmic Potentials of Hydra,” *Proc. Natl. Acad. Sci. U. S. A.*, vol. 48, no. 8, pp. 1376–1382, Aug. 1962.

[39] R. K. Josephson and M. Macklin, “Electrical Properties of the Body Wall of Hydra,” *J. Gen. Physiol.*, vol. 53, no. 5, pp. 638–665, May 1969.

[40] T.-W. Chen *et al.*, “Ultrasensitive fluorescent proteins for imaging neuronal activity,” *Nature*, vol. 499, no. 7458, pp. 295–300, Jul. 2013.

[41] T. Jegla, H. Q. Marlow, B. Chen, D. K. Simmons, S. M. Jacobo, and M. Q. Martindale, “Expanded Functional Diversity of Shaker K+ Channels in Cnidarians Is Driven by Gene Expansion,” *PLOS ONE*, vol. 7, no. 12, p. e51366, Dec. 2012.

[42] Y. Moran and H. H. Zakon, “The Evolution of the Four Subunits of Voltage-Gated Calcium Channels: Ancient Roots, Increasing Complexity, and Multiple Losses,” *Genome Biol. Evol.*, vol. 6, no. 9, pp. 2210–2217, Aug. 2014.

[43] Y. Moran, M. G. Barzilai, B. J. Liebeskind, and H. H. Zakon, “Evolution of voltage-gated ion channels at the emergence of Metazoa,” *J. Exp. Biol.*, vol. 218, no. 4, pp. 515–525, Feb. 2015.

[44] J. D. Spafford, A. N. Spencer, and W. J. Gallin, “A putative voltage-gated sodium channel alpha subunit (PpSCN1) from the hydrozoan jellyfish, Polyorchis penicillatus: structural comparisons and evolutionary considerations,” *Biochem. Biophys. Res. Commun.*, vol. 244, no. 3, pp. 772–780, Mar. 1998.

[45] J. Spafford, N. Grigoriev, and A. Spencer, “Pharmacological properties of voltage-gated Na+ currents in motor neurones from a hydrozoan jellyfish Polyorchis penicillatus,” *J. Exp. Biol.*, vol. 199, no. 4, pp. 941–948, Apr. 1996.

[46] M. G. Barzilai *et al.*, “Convergent Evolution of Sodium Ion Selectivity in Metazoan Neuronal Signaling,” *Cell Rep.*, vol. 2, no. 2, pp. 242–248, Aug. 2012.

[47] G. O. Mackie and R. W. Meech, “Separate sodium and calcium spikes in the same axon,” *Nature*, vol. 313, no. 6005, pp. 791–793, Feb. 1985.

[48] S. Gao and M. Zhen, “Action potentials drive body wall muscle contractions in Caenorhabditis elegans,” *Proc. Natl. Acad. Sci.*, vol. 108, no. 6, pp. 2557–2562, Feb. 2011.

[49] E. C. Baker *et al.*, “Functional Characterization of Cnidarian HCN Channels Points to an Early Evolution of Ih,” *PLOS ONE*, vol. 10, no. 11, p. e0142730, Nov. 2015.

[50] P. Pierobon, “Coordinated modulation of cellular signaling through ligand-gated ion channels in Hydra vulgaris (Cnidaria, Hydrozoa),” *Int. J. Dev. Biol.*, vol. 56, no. 6-7–8, pp. 551–565, 2012.

[51] J. A. Chapman *et al.*, “The dynamic genome of Hydra,” *Nature*, vol. 464, no. 7288, pp. 592–596, Mar. 2010.

[52] C. Collin *et al.*, “Two types of muscarinic acetylcholine receptors in <Emphasis Type="Italic">Drosophila</Emphasis> and other arthropods,” *Cell. Mol. Life Sci.*, vol. 70, no. 17, pp. 3231–3242, Sep. 2013.

[53] T. Takahashi and N. Hamaue, “Molecular characterization of Hydra acetylcholinesterase and its catalytic activity,” *FEBS Lett.*, vol. 584, no. 3, pp. 511–516, Feb. 2010.

[54] T. Fujisawa, “Hydra Peptide Project 1993–2007,” *Dev. Growth Differ.*, vol. 50, no. s1, pp. S257–S268, Jun. 2008.

[55] S. Yum *et al.*, “A Novel Neuropeptide, Hym-176, Induces Contraction of the Ectodermal Muscle in Hydra,” *Biochem. Biophys. Res. Commun.*, vol. 248, no. 3, pp. 584–590, Jul. 1998.

[56] Hayakawa Eisuke, Takahashi Toshio, Nishimiya-Fujisawa Chiemi, and Fujisawa Toshitaka, “A novel neuropeptide (FRamide) family identified by a peptidomic approach in Hydra magnipapillata,” *FEBS J.*, vol. 274, no. 20, pp. 5438–5448, Sep. 2007.

[57] T. Takahashi *et al.*, “Identification of a new member of the GLWamide peptide family: physiological activity and cellular localization in cnidarian polyps,” *Comp. Biochem. Physiol. B Biochem. Mol. Biol.*, vol. 135, no. 2, pp. 309–324, Jun. 2003.

[58] S. Dürrnagel *et al.*, “Three Homologous Subunits Form a High Affinity Peptide-gated Ion Channel in Hydra,” *J. Biol. Chem.*, vol. 285, no. 16, pp. 11958–11965, Apr. 2010.

[59] S. Gründer and M. Assmann, “Peptide-gated ion channels and the simple nervous system of Hydra,” *J. Exp. Biol.*, vol. 218, no. 4, pp. 551–561, Feb. 2015.

[60] M. Assmann, A. Kuhn, S. Dürrnagel, T. W. Holstein, and S. Gründer, “The comprehensive analysis of DEG/ENaC subunits in Hydra reveals a large variety of peptide-gated channels, potentially involved in neuromuscular transmission,” *BMC Biol.*, vol. 12, no. 1, p. 84, Oct. 2014.

[61] T. Fujisawa and E. Hayakawa, “Peptide signaling in Hydra,” *Int. J. Dev. Biol.*, vol. 56, no. 6-7–8, pp. 543–550, Jun. 2012.

[62] D. Sher, Y. Fishman, N. Melamed-Book, M. Zhang, and E. Zlotkin, “Osmotically driven prey disintegration in the gastrovascular cavity of the green hydra by a pore-forming protein,” *FASEB J.*, vol. 22, no. 1, pp. 207–214, Aug. 2007.

[63] D. Sher *et al.*, “Hydralysins, a New Category of β-Pore-forming Toxins in Cnidaria,” *J. Biol. Chem.*, vol. 280, no. 24, pp. 22847–22855, Jun. 2005.

[64] Y. J. M. Liew, W. T. Soh, W. F. Jiemy, and J. S. Hwang, “Mutagenesis and functional analysis of the pore-forming toxin HALT-1 from Hydra magnipapillata,” *Toxins*, vol. 7, no. 2, pp. 407–422, Feb. 2015.

[65] “Gland cells arise by differentiation from interstitial cells in Hydra attenuata - ScienceDirect.” [Online]. Available: https://www.sciencedirect.com/science/article/pii/0012160687903216?via%3Dihub. [Accessed: 08-May-2018].

[66] T. Schmidt and C. N. David, “Gland cells in Hydra: cell cycle kinetics and development,” *J. Cell Sci.*, vol. 85, no. 1, pp. 197–215, Sep. 1986.

[67] W. M. Kier, “The diversity of hydrostatic skeletons,” *J. Exp. Biol.*, vol. 215, no. 8, pp. 1247–1257, Apr. 2012.

[68] R. K. Josephson and M. Macklin, “Transepithelial potentials in Hydra,” *Science*, vol. 156, no. 3782, pp. 1629–1631, Jun. 1967.

[69] V. A. Canfield, K. Y. Xu, T. D’Aquila, A. W. Shyjan, and R. Levenson, “Molecular cloning and characterization of Na,K-ATPase from Hydra vulgaris: implications for enzyme evolution and ouabain sensitivity,” *New Biol.*, vol. 4, no. 4, pp. 339–348, Apr. 1992.

[70] R. D. Prusch, D. J. Benos, and M. Ritter, “Osmoregulatory control mechanisms in freshwater coelenterates,” *Comp. Biochem. Physiol. A Physiol.*, vol. 53, no. 2, pp. 161–164, Jan. 1976.

[71] A.-M. Hartmann, L. I. Pisella, I. Medina, and H. G. Nothwang, “Molecular cloning and biochemical characterization of two cation chloride cotransporter subfamily members of Hydra vulgaris,” *PLOS ONE*, vol. 12, no. 6, p. e0179968, Jun. 2017.

[72] D. J. Benos, R. G. Kirk, W. P. Barba, and M. M. Goldner, “Hyposmotic fluid formation in Hydra,” *Tissue Cell*, vol. 9, no. 1, pp. 11–22, Jan. 1977.

[73] D. J. Benos and R. D. Prusch, “Osmoregulation in Hydra: Column contraction as a function of external osmolality,” *Comp. Biochem. Physiol. A Physiol.*, vol. 44, no. 4, pp. 1397–1400, Apr. 1973.

[74] R. D. Campbell, “Structure of the mouth of <Emphasis Type="Italic">Hydra</Emphasis> spp. A breach in the epithelium that disappears when it closes,” *Cell Tissue Res.*, vol. 249, no. 1, pp. 189–197, Jul. 1987.

[75] H. Shimizu, Y. Takaku, X. Zhang, and T. Fujisawa, “The aboral pore of hydra: evidence that the digestive tract of hydra is a tube not a sac,” *Dev. Genes Evol.*, vol. 217, no. 8, pp. 563–568, Aug. 2007.

[76] M. Macklin, T. Roma, and K. Drake, “Water Excretion by Hydra,” *Science*, vol. 179, no. 4069, pp. 194–195, Jan. 1973.

[77] R. Yuste, “From the neuron doctrine to neural networks,” *Nat. Rev. Neurosci.*, vol. 16, no. 8, pp. 487–497, Aug. 2015.

[78] T. J. Herron, P. Lee, and J. Jalife, “Optical Imaging of Voltage and Calcium in Cardiac Cells & Tissues,” *Circ. Res.*, vol. 110, no. 4, pp. 609–623, Feb. 2012.

[79] A. P. Baader, L. Büchler, L. Bircher-Lehmann, and A. G. Kléber, “Real time, confocal imaging of Ca2+ waves in arterially perfused rat hearts,” *Cardiovasc. Res.*, vol. 53, no. 1, pp. 105–115, Jan. 2002.

[80] A. A. Gharibans, S. Kim, D. C. Kunkel, and T. P. Coleman, “High-Resolution Electrogastrogram: A Novel, Noninvasive Method for Determining Gastric Slow-Wave Direction and Speed,” *IEEE Trans. Biomed. Eng.*, vol. 64, no. 4, pp. 807–815, Apr. 2017.

[81] R. E. Dixon *et al.*, “Electrical Slow Waves in the Mouse Oviduct Are Dependent upon a Calcium Activated Chloride Conductance Encoded by Tmem16a,” *Biol. Reprod.*, vol. 86, no. 1, Jan. 2012.

[82] S. Torihashi, T. Fujimoto, C. Trost, and S. Nakayama, “Calcium Oscillation Linked to Pacemaking of Interstitial Cells of Cajal REQUIREMENT OF CALCIUM INFLUX AND LOCALIZATION OF TRP4 IN CAVEOLAE,” *J. Biol. Chem.*, vol. 277, no. 21, pp. 19191–19197, May 2002.

[83] J. F. Griffith, “Functional imaging of the musculoskeletal system,” *Quant. Imaging Med. Surg.*, vol. 5, no. 3, pp. 323–331, Jun. 2015.

[84] J. Vergara, M. DiFranco, D. Compagnon, and B. A. Suarez-Isla, “Imaging of calcium transients in skeletal muscle fibers.,” *Biophys. J.*, vol. 59, no. 1, pp. 12–24, Jan. 1991.

[85] A. Tsugorka, E. Rios, and L. A. Blatter, “Imaging elementary events of calcium release in skeletal muscle cells,” *Science*, vol. 269, no. 5231, pp. 1723–1726, Sep. 1995.

[86] R. Kerr, V. Lev-Ram, G. Baird, P. Vincent, R. Y. Tsien, and W. R. Schafer, “Optical Imaging of Calcium Transients in Neurons and Pharyngeal Muscle of C. elegans,” *Neuron*, vol. 26, no. 3, pp. 583–594, Jun. 2000.

[87] S. Shimozono, T. Fukano, K. D. Kimura, I. Mori, Y. Kirino, and A. Miyawaki, “Slow Ca2+ dynamics in pharyngeal muscles in Caenorhabditis elegans during fast pumping,” *EMBO Rep.*, vol. 5, no. 5, pp. 521–526, May 2004.

[88] S. I. Shyn, R. Kerr, and W. R. Schafer, “Serotonin and Go Modulate Functional States of Neurons and Muscles Controlling C. elegans Egg-Laying Behavior,” *Curr. Biol.*, vol. 13, no. 21, pp. 1910–1915, Oct. 2003.

[89] S. Sponberg, T. L. Daniel, and A. L. Fairhall, “Dual Dimensionality Reduction Reveals Independent Encoding of Motor Features in a Muscle Synergy for Insect Flight Control,” *PLOS Comput. Biol.*, vol. 11, no. 4, p. e1004168, Apr. 2015.

[90] F.-O. Lehmann, D. A. Skandalis, and R. Berthé, “Calcium signalling indicates bilateral power balancing in the Drosophila flight muscle during manoeuvring flight,” *J. R. Soc. Interface*, vol. 10, no. 82, May 2013.

[91] J. Wittlieb, K. Khalturin, J. U. Lohmann, F. Anton-Erxleben, and T. C. G. Bosch, “Transgenic Hydra allow in vivo tracking of individual stem cells during morphogenesis,” *Proc. Natl. Acad. Sci.*, vol. 103, no. 16, pp. 6208–6211, Apr. 2006.

[92] H. Dana *et al.*, “Sensitive red protein calcium indicators for imaging neural activity,” *eLife*, vol. 5, p. e12727, Mar. 2016.

[93] C. E. Dana, K. M. Glauber, T. A. Chan, D. M. Bridge, and R. E. Steele, “Incorporation of a Horizontally Transferred Gene into an Operon during Cnidarian Evolution,” *PLOS ONE*, vol. 7, no. 2, p. e31643, Feb. 2012.

[94] C. E. Juliano, H. Lin, and R. E. Steele, “Generation of Transgenic Hydra by Embryo Microinjection,” *JoVE J. Vis. Exp.*, no. 91, pp. e51888–e51888, Sep. 2014.

[95] E. N. Browne, “The production of new hydranths in Hydra by the insertion of small grafts,” *J. Exp. Zool.*, vol. 7, no. 1, pp. 1–23, Aug. 1909.

[96] L. Muscatine, *Coelenterate Biology: Reviews and New Perspectives*. Elsevier, 2012.

[97] W. F. Loomis, “Glutathione Control of the Specific Feeding Reactions of Hydra,” *Ann. N. Y. Acad. Sci.*, vol. 62, no. 9, pp. 211–227.

[98] J. Shi and C. Tomasi, “Good features to track,” in *1994 Proceedings of IEEE Conference on Computer Vision and Pattern Recognition*, 1994, pp. 593–600.

[99] C. Tomasi and T. Kanade, “Detection and Tracking of Point Features,” International Journal of Computer Vision, 1991.

[100] B. D. Lucas and T. Kanade, “An Iterative Image Registration Technique with an Application to Stereo Vision,” in *Proceedings of the 7th International Joint Conference on Artificial Intelligence - Volume 2*, San Francisco, CA, USA, 1981, pp. 674–679.

[101] Greenwood M., “On Digestion in Hydra, with some Observations on the Structure of the Endoderm,” *J. Physiol.*, vol. 9, no. 5–6, pp. 317–344, Dec. 1888.

[102] A. Böttger *et al.*, “Horizontal Gene Transfer Contributed to the Evolution of Extracellular Surface Structures: The Freshwater Polyp Hydra Is Covered by a Complex Fibrous Cuticle Containing Glycosaminoglycans and Proteins of the PPOD and SWT (Sweet Tooth) Families,” *PLOS ONE*, vol. 7, no. 12, p. e52278, Dec. 2012.

[103] Y. Wenger, W. Buzgariu, S. Reiter, and B. Galliot, “Injury-induced immune responses in Hydra,” *Semin. Immunol.*, vol. 26, no. 4, pp. 277–294, Aug. 2014.

[104] T. C. G. Bosch, “Rethinking the role of immunity: lessons from Hydra,” *Trends Immunol.*, vol. 35, no. 10, pp. 495–502, Oct. 2014.

[105] R. Aufschnaiter, R. Wedlich-Söldner, X. Zhang, and B. Hobmayer, “Apical and basal epitheliomuscular F-actin dynamics during Hydra bud evagination,” *Biol. Open*, vol. 6, no. 8, p. 1137, Aug. 2017.

[106] W. Buzgariu, S. A. Haddad, S. Tomczyk, Y. Wenger, and B. Galliot, "Multi-functionality and plasticity characterize epithelial cells in Hydra," *Tissue Barriers*, vol. 3, no. 4, p. e1068908, Oct. 2015.

[107] R. D. Campbell, R. K. Josephson, W. E. Schwab, and N. B. Rushforth, "Excitability of nerve-free hydra," *Nature*, vol. 262, no. 5567, pp. 388–390, Jul. 1976.

[108] D. F. van Helden and M. S. Imtiaz, "Ca2+ phase waves: a basis for cellular pacemaking and long-range synchronicity in the guinea-pig gastric pylorus," *J. Physiol.*, vol. 548, no. Pt 1, pp. 271–296, Apr. 2003.

[109] D. F. Van Helden, M. S. Imtiaz, K. Nurgaliyeva, P.-Y. von der Weid, and P. J. Dosen, "Role of calcium stores and membrane voltage in the generation of slow wave action potentials in guinea-pig gastric pylorus," *J. Physiol.*, vol. 524, no. Pt 1, pp. 245–265, Apr. 2000.

[110] H. Ozaki, R. J. Stevens, D. P. Blondfield, N. G. Publicover, and K. M. Sanders, "Simultaneous measurement of membrane potential, cytosolic Ca2+, and tension in intact smooth muscles," *Am. J. Physiol.-Cell Physiol.*, vol. 260, no. 5, pp. C917–C925, May 1991.

[111] W. J. E. P. Lammers, B. Stephen, J. R. Slack, and S. Dhanasekaran, "Anisotropic propagation in the small intestine," *Neurogastroenterol. Motil.*, vol. 14, no. 4, pp. 357–364, Aug. 2002.

[112] G. W. Dorn and T. Force, "Protein kinase cascades in the regulation of cardiac hypertrophy," *J. Clin. Invest.*, vol. 115, no. 3, pp. 527–537, Mar. 2005.

[113] N. C. Salazar, J. Chen, and H. A. Rockman, "Cardiac GPCRs: GPCR signaling in healthy and failing hearts," *Biochim. Biophys. Acta BBA - Biomembr.*, vol. 1768, no. 4, pp. 1006–1018, Apr. 2007.

[114] B. M. Wynne, C.-W. Chiao, and R. C. Webb, "Vascular smooth muscle cell signaling mechanisms for contraction to angiotensin II and endothelin-1," *J. Am. Soc. Hypertens.*, vol. 3, no. 2, pp. 84–95, Mar. 2009.

[115] G. Shibley, "Gastrodermal contractions correlated with rhythmic potentials and prelocomotor bursts in Hydra," *Am. Zool.*, vol. 9, no. 3, p. 586, 1969.

[116] Hodgkin A. L. and Keynes R. D., "Movements of labelled calcium in squid giant axons," *J. Physiol.*, vol. 138, no. 2, pp. 253–281, Sep. 1957.

[117] A. Trewavas, "Le Calcium, C'est la Vie: Calcium Makes Waves," *Plant Physiol.*, vol. 120, no. 1, pp. 1–6, May 1999.

[118] R. K. P. Benninger, M. Zhang, W. S. Head, L. S. Satin, and D. W. Piston, "Gap Junction Coupling and Calcium Waves in the Pancreatic Islet," *Biophys. J.*, vol. 95, no. 11, pp. 5048–5061, Dec. 2008.

[119] M. F. Leite, A. D. Burgstahler, and M. H. Nathanson, "Ca2+ waves require sequential activation of inositol trisphosphate receptors and ryanodine receptors in pancreatic acini," *Gastroenterology*, vol. 122, no. 2, pp. 415–427, Feb. 2002.

[120] J. Sneyd, K. Tsaneva-Atanasova, J. I. E. Bruce, S. V. Straub, D. R. Giovannucci, and D. I. Yule, “A model of calcium waves in pancreatic and parotid acinar cells,” *Biophys. J.*, vol. 85, no. 3, pp. 1392–1405, Sep. 2003.

[121] G. C. Amberg and M. F. Navedo, “Calcium dynamics in vascular smooth muscle,” *Microcirc. N. Y. N 1994*, vol. 20, no. 4, pp. 281–289, May 2013.

[122] W.-G. Choi, M. Toyota, S.-H. Kim, R. Hilleary, and S. Gilroy, “Salt stress-induced Ca2+ waves are associated with rapid, long-distance root-to-shoot signaling in plants,” *Proc. Natl. Acad. Sci.*, vol. 111, no. 17, pp. 6497–6502, Apr. 2014.

[123] R. N. Finn, F. Chauvigné, J. B. Hlidberg, C. P. Cutler, and J. Cerdà, “The Lineage-Specific Evolution of Aquaporin Gene Clusters Facilitated Tetrapod Terrestrial Adaptation,” *PLOS ONE*, vol. 9, no. 11, p. e113686, Nov. 2014.

[124] H. M. Lenhoff, *Hydra: research methods*. Plenum Press, 1983.

[125] N. Otsu, “A Threshold Selection Method from Gray-Level Histograms,” *IEEE Trans. Syst. Man Cybern.*, vol. 9, no. 1, pp. 62–66, Jan. 1979.

[126] “PackIO and EphysViewer: software tools for acquisition and analysis of neuroscience data | bioRxiv.” [Online]. Available: https://www.biorxiv.org/content/early/2016/05/18/054080. [Accessed: 16-May-2018].

APPENDIX

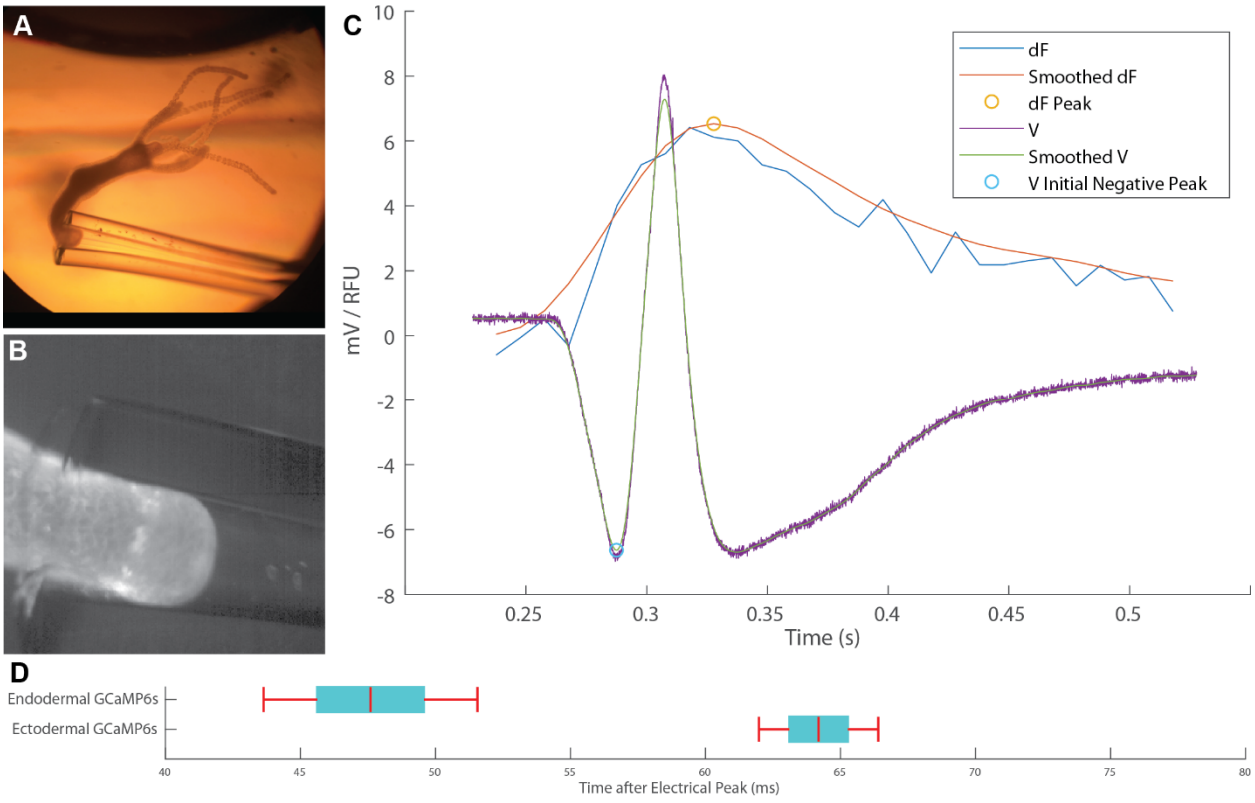

Figure 18: Suction electrode recordings align recordings made with different indicators

A) Hydra mounted in the electrode
B) Example frame from calcium imaging
C) Example electrophysiological trace (V) plotted against first derivative of fluorescence trace (dF), with peaks identified
D) Measured delays of calcium influx peaks in endoderm and ectoderm versus initial negative peak of electrophysiological trace

A)

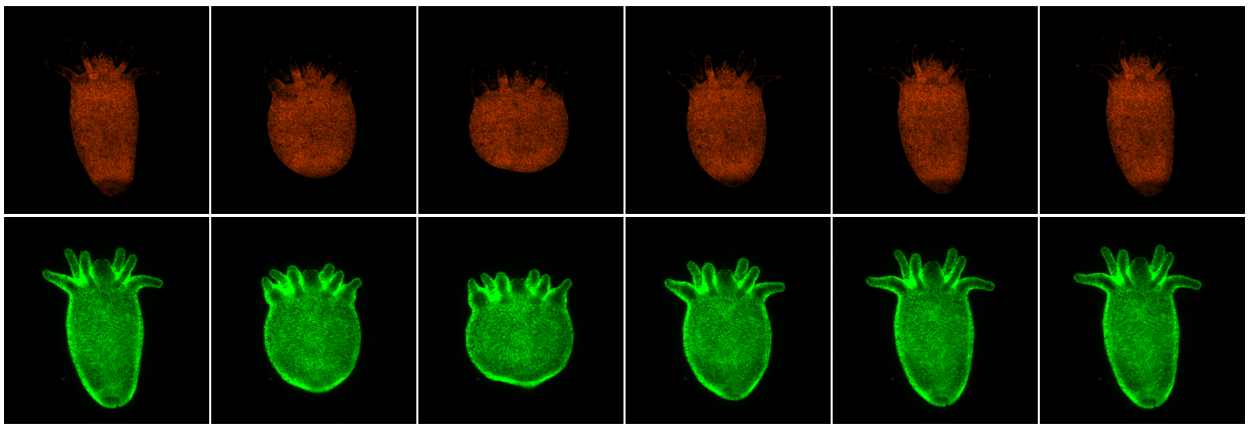

B)

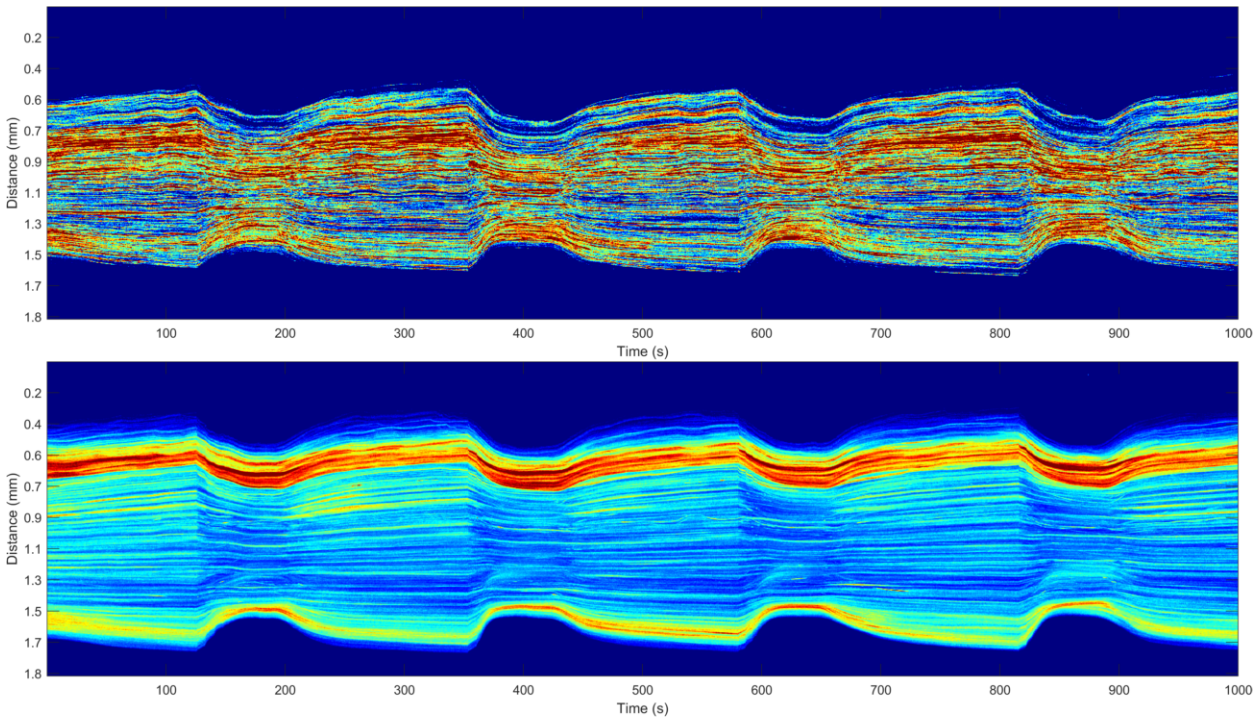

Figure 19: Static fluorophore control

A contraction burst was recorded using a hydra expressing fluorescent proteins DsRed2 and EGFP in place of calcium indicators. A) Keyframes showing fluorescence images of polyp at various stages of contraction B) Kymographs show that the changes in fluorescence show in calcium movies clearly arise from calcium dynamics rather than tissue compression.